Mechanistic Insights into Manganese Induced Down-regulation of the *Cis* Golgi Glycoprotein GPP130

by

Ritika Tewari

A thesis submitted in partial fulfillment of the requirements
for the degree of
Doctor of Philosophy in the field of Biological Sciences

Department of Biological Sciences
Carnegie Mellon University
Pittsburgh, Pennsylvania

May 7, 2015

Thesis Advisor: Dr. Adam D. Linstedt

ABSTRACT

During invasion of host cells the *Shigella* bacterial toxin sorts away from degradative lysosomes and traffics to the Golgi complex by binding the cycling transmembrane protein GPP130 as GPP130 returns from endosomes to the Golgi. Remarkably, an increase in Golgi manganese (Mn) alters the trafficking of GPP130 causing its degradation in lysosomes thereby protecting cells against lethal doses of purified toxin. Mn-induced down-regulation of GPP130 is thus an important paradigm for therapy against the incurable Shiga toxicosis as well as metal-regulated protein sorting in the Golgi. The experiments herein reveal significant aspects of the mechanism. We identified a transferable trafficking determinant within the GPP130 lumenal stem domain that bound Mn and observed that Mn binding induced its oligomerization in the Golgi. Significantly, alanine substitutions that blocked Mn binding abrogated both oligomerization and GPP130 sorting to lysosomes. GPP130 oligomers engaged the canonical Golgi-lysosomal trafficking machinery, as GPP130 exit from the Golgi required the sorting adaptor GGA1 and the clathrin vesicle coat complex. Surprisingly, oligomerization was sufficient since GPP130 redistributed to lysosomes in the absence of Mn by forced aggregation using a drug-controlled self-interacting version of the FKBP domain. Further, neither the cytoplasmic domain nor residues in the lumenal stem domain critical for normal GPP130 cycling were required for this redistribution. These observations suggested that higher order oligomerization might generally cause lysosomal targeting of Golgi membrane proteins. Indeed, induced oligomerization of two other unrelated Golgi proteins caused their redistribution to endosome/lysosome-like punctae and subsequent degradation. The ER-based unfolded protein response was not activated during this process. Altogether, these results show that Mn binds and oligomerizes GPP130 targeting it to what may be a pre-existing quality control pathway in the Golgi where aggregated proteins are degraded in lysosomes.

ACKNOWLEDGEMENTS

I would like to extend a grateful thanks to my advisor, Dr. Adam D. Linstedt for his constant support and guidance during the course of my PhD. I am a better scientist today because of his faith in my abilities. His scientific acumen, tenacity and kindness have inspired me during my time in the lab and will continue to inspire me for many more years to come.

I would like to thank Dr. Somshuvra Mukhopadhyay immensely for being a very patient mentor during my first few years in the lab. The basic cell biology techniques I learnt from him provided a strong foundation to build my thesis and contributed very strongly to my growth as a scientist.

I would like to thank my committee members, Dr. Manoj A. Puthenveedu and Dr. David Hackney for their expert feedback, advice and encouragement. I have learnt a lot from our committee meetings, which played a key role in shaping my thesis project. Thank you, Dr. Jeffrey Brodsky for agreeing to be the external member on my committee and for your feedback on my project during the local traffic symposiums.

I would like to thank the past members of the Linstedt lab- Dr. Debrup Sengupta, Dr. Smita Yadav, Dr. Timothy Jarvela and Cassandra Priddy for being outstanding seniors to emulate and learn from.

I would like to acknowledge the present members of the Linstedt lab- Collin Bachert, Steve Truschel, Swati Venkat, Emily Simon and Lina Song for their support, engaging discussions and providing an encouraging environment for scientific pursuits.

I would also like to thank Dr. Tina Lee and members of the Lee and Puthenveedu labs for their feedback and insightful discussions during lab meetings.

Finally, I would like to express my gratitude towards my parents, sister and husband. In spite of the distance of thousands of miles, they have been an integral part of all my accomplishments and failures during my graduate studies. If it were not for their unwavering support, I would not have been here. I would like to thank my family for believing nothing is beyond my reach and for their selfless and unconditional love and support.

TABLE OF CONTENTS

Chapter 1: Introduction

Chapter 2: Manganese induces Oligomerization to Promote the Down-regulation of GPP130-the Intracellular Trafficking Receptor used by Shiga Toxin

Chapter 3: Induced-Oligomerization Targets Golgi proteins for Degradation in Lysosomes

Chapter 4: Conclusions and Future Directions

LIST OF FIGURES

Chapter 1: Introduction

Chapter 2: Manganese induces Oligomerization to Promote the Down-regulation of GPP130-the Intracellular Trafficking Receptor used by Shiga Toxin

Chapter 3: Induced-Oligomerization Targets Golgi proteins for Degradation in Lysosomes

CHAPTER 1

INTRODUCTION

This thesis concerns the mechanism by which manganese (Mn) down-regulates the cycling membrane protein GPP130, which is the basis of a potential therapy against Shiga toxicosis. Because the down-regulation occurs by altering GPP130 trafficking in the trans Golgi network, this chapter briefly introduces Shiga toxicosis (1.1) and then provides background on Mn and metal-regulated protein trafficking (1.2) and protein sorting at the trans Golgi network (1.3). The chapter closes with a review of GPP130 trafficking (1.4).

1.1 Therapy against Shiga toxicosis

Shiga toxin belongs to the notorious class of AB_5 toxins, examples of which include the well known infectious exotoxins- cholera and pertussis, that follow an elaborate retrograde trafficking pathway to cause intracellular infection (Sandvig et al., 2004). Shiga toxin-producing bacteria of the *Shigella* genus and enterohemorrhagic *Escherichia coli* (EHEC) species infect more than 150 million individuals each year and cause more than a million deaths from life threatening diarrhea, dysentery, hemorrhagic colitis, and hemorrhagic uremic syndrome (Beddoe et al., 2010). Treatment options, mostly involving hydration, are extremely limited and mainly symptomatic.

Shiga toxin, like other AB_5 toxins, consists of a catalytic A subunit and homopentameric B subunit which mediates its membrane trafficking (Johaness and Wunder, 2011). As the toxin invades the host cell, its B subunit associates with the cell

surface receptor, glycosphingolipid GB3, to internalize the toxin to early endosomes. Shiga toxin avoids lysosomal degradation by sorting into endosomal membrane tubules that move directly to the Golgi (Johannes and Wunder, 2011). For two major isoforms of Shiga toxin, STx (present in *Shigella*) and STx1 (present in strains of *E. coli*), sorting into these endosomal tubules is mediated by binding to the host-cell transmembrane protein, GPP130, in early endosomes. In mammalian cells, GPP130 is localized to the *cis* Golgi at steady state and constitutively cycles between the Golgi and endosomes. STx/STx1 directly binds to a site in the lumenal stem domain of GPP130, close to the cell membrane (Mukhopadhyay and Linstedt, 2012). In this way it is thought that STx/STx1 piggybacks a ride to the Golgi directly from endosomes by cleverly utilizing the late endosome/lysosome-bypass pathway to escape lysosomal degradation. From the Golgi, the toxin traffics to the endoplasmic reticulum where the A subunit translocates into the cytosol to inactivate ribosomes by attacking the 28S ribosomal RNA of the 60S ribosomal subunit (Endo et al., 1988, Fraser et al., 1994).

Blocking the direct endosome-Golgi trafficking of STx/STx1 is therapeutically attractive since inhibiting transport at this step diverts the toxin to lysosomes for degradation and clears any residual toxin from infected cells. Remarkably, relatively moderate increases in Golgi Mn levels result in the lysosomal degradation of GPP130. In the absence of GPP130, STx/STx1 is re-routed to the lysosomes thereby clearing infection from the cell (Mukhopadhyay et al., 2012). Indeed, non-toxic doses of Mn have been shown to effectively protect against STx/STx1-induced toxicity and death in both cell culture and a mouse model (Mukhopadhyay et al., 2012). Thus, by down-regulating GPP130, Mn can potentially serve as a readily available and cheap small-molecule

inhibitor of STx/STx1.

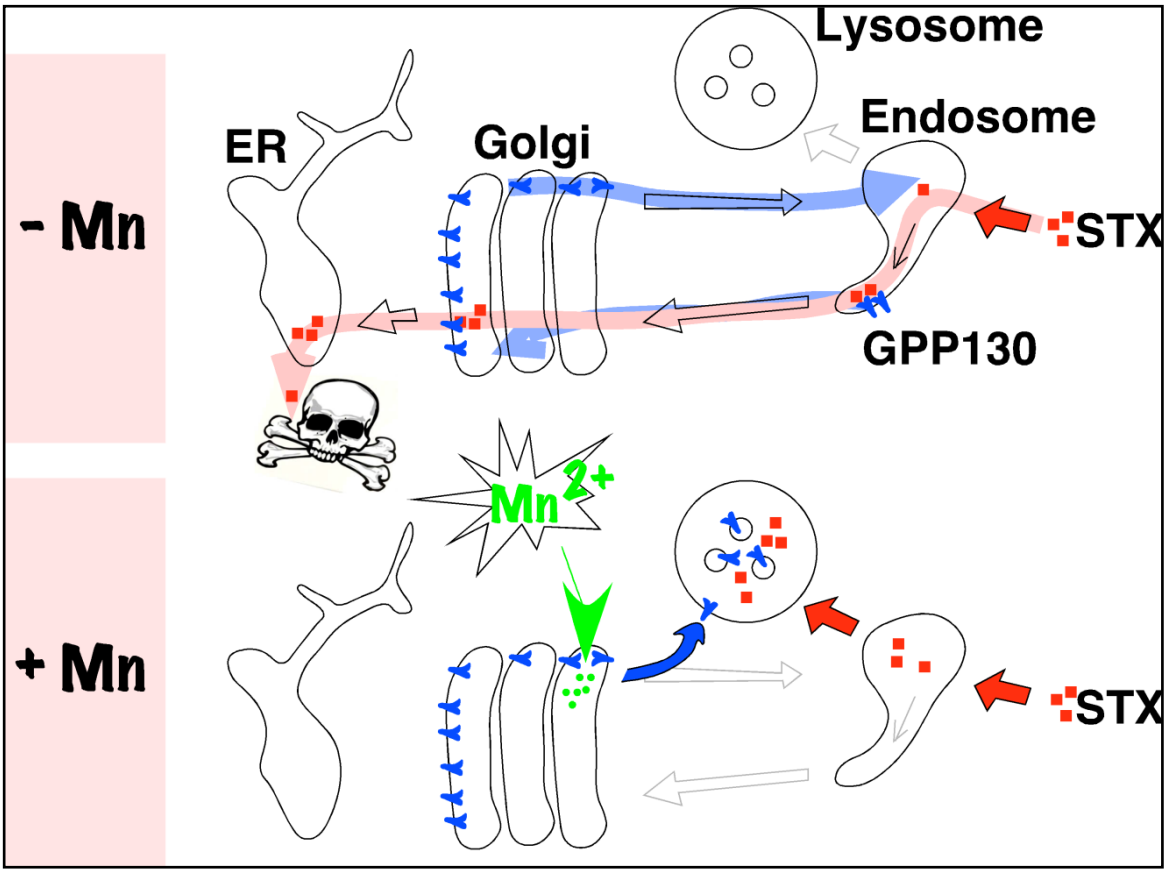

Figure 1-1. Schematic Model showing GPP130 and STx trafficking in mammalian cells in the presence and absence of Mn.

In control cells (-Mn), the Golgi-to-endosome cycling of GPP130 is depicted in blue and the GPP130-dependent retrograde trafficking of Shiga toxin (STx) via the late endosome/lysosome-bypass pathway is depicted in red. Mn addition (+Mn) diverts GPP130 to lysosomes leaving STx no trafficking receptor for sorting into Golgi-directed endosome tubules. As a result, STx is degraded in lysosomes and cleared from the cell. (Adapted from Mukhopadhyay et al., 2012).

1.2 Metal-regulated protein trafficking

Metal ions are important for normal cellular processes, but toxic at elevated levels

Essential divalent metal ions, such as copper (Cu), manganese (Mn), iron (Fe) play important roles in many cellular processes vital for human health. For instance, Mn acts as a cofactor to a variety of essential enzymes such as superoxide dismutase that plays a role in preventing cellular oxidative stress, arginase that plays a role in urea production in the liver, DNA and RNA polymerases, and Golgi enzymes required for N-linked glycosylation (Crossgrove and Zheng, 2004). In the brain, Mn has been shown to associate with the astrocyte specific enzyme glutamine synthetase and plays a role in metabolism of brain glutamate to glutamine (Takeda et al., 1995).

While crucial for normal cellular processes, elevated cellular levels of these metal ions are toxic and cause life-threatening diseases, thus highlighting the importance of the study of ion homeostasis. For instance, at toxic cellular levels, Mn competes with magnesium binding sites in proteins, fragments the Golgi, delays soluble and membrane-bound protein secretion, disrupts mitochondrial function and eventually causes apoptosis (Towler et al., 2000). Mn cytotoxicity develops into a progressive disorder of the extrapyramidal system similar to Parkinson's disease, manganism, common in occupationally exposed miners, welders and smelters (Olanow, 2004; Crossgrove and Zheng, 2004). Manganism is associated with the preferential degeneration of GABAminergic neurons within the globus pallidus causing neurological symptoms of reduced response speed, mood swings, compulsive behavior and intellectual deficits during the early stages of the disease. Protracted exposure leads to

more permanent and irreversible extrapyramidal disfunction resembling Parkinson's disease (Roth et al., 2002). Classic symptoms include masklike face, limb rigidity, mild tremors, bradykinesia, dystonia, slurred speech and disturbance of balance (Olanow, 2004). Even though many treatments are now available to combat Parkinson's disease, there currently are no known treatments for manganism, highlighting the importance for understanding ion homeostasis.

Divalent metal ions and altered protein sorting

Although the field of mammalian ion homeostasis is burgeoning, a lot of fundamental questions still remain unanswered. Chief among them is how proteins involved in ion homeostasis sense the metal ion and respond to its altered levels? Divalent metals ions have been well documented to alter the sorting of membrane proteins in mammalian cells, however, not much is known about the mechanism of metal-regulated change in protein sorting. For instance, copper (Cu) homeostasis in mammalian cells involves the Cu transporters, P-type ATPases- ATP7A and ATP7B, to sense and respond to cellular Cu levels. These transporters provide Cu to cuproenzymes as well as maintain Cu homeostasis (La Fontaine and Mercer, 2007). Cytosolic levels of Cu determine the sorting of these ATPases at the trans Golgi network (TGN). Under physiological levels of Cu, the ATPases are localized to the TGN to supply Cu to cuproenzymes in the secretory pathway (La Fontaine and Mercer, 2007). In response to elevated Cu levels, they move to the plasma membrane to facilitate the elimination of excess Cu. Consequently, Wilson's disease, an autosomal recessive disorder caused by mutations in ATP7B gene, is associated with impediment in Cu disposal, leading to marked Cu accumulation in the hepatocytes and culminating in liver failure (Lalioti et al., 2008).

Despite disease relevance, the molecular mechanism mediating translocation of these ATPases from TGN to the plasma membrane in response to elevated Cu levels is poorly understood and only scattered evidence is available. However, regardless of the gaps in full understanding of the mechanism of TGN retention and trafficking to post-Golgi compartments, it is believed that interaction of Cu with these ATPases stabilizes a conformation primed for Golgi export and sorting to post-Golgi targets (Polishchuk et al., 2013).

Mn-induced trafficking in *Saccharomyces cerevisiae*

In the case of Mn, much of the current knowledge about pathways of Mn-regulated trafficking has emerged from molecular genetic studies in *Saccharomyces cerevisiae*. Pathways of manganese trafficking in yeast strike a delicate balance between two objectives: to ensure proper delivery of the ion to the target Mn-requiring enzymes in the cytosol, Golgi and mitochondria (manganese utilization pathways) and to prevent accumulation of Mn in the freely reactive form (manganese detoxification pathways).

Extracellular Mn can enter yeast cells via a number of ion transporters. Two such widely studied transporters, Smf1p and Smf2p, belong to the Nramp (Natural resistance associated macrophage protein) family of metal ion transporters and are functionally non-redundant (Luk et al., 2003). These metal-proton symporters act on a broad range of divalent metals, including Mn, Fe, cadmium (Cd), and Cu. Smf1p is a high affinity transporter for Mn localized to the plasma membrane (Supek et al., 1996, 1997), while Smf2p is localized to intracellular Golgi-like vesicles (Luk et al., 2003). Smf2p containing vesicles function as storage depots or transient passage stations for Mn (Culotta et al., 2005). The Mn transported into the yeast cell is then delivered to the Golgi via the P-type

ATPase, Pmr1p (plasma membrane ATPase–related transporter for both Ca and Mn; Durr et al., 1998) and the mitochondria via an unknown transporter for activation of Mn-dependent enzymes (Jensen et al., 2014).

Smf1p and Smf2p exhibit multiple levels of post-translational regulation in response to changes in Mn concentration. Under physiological conditions of sufficient Mn, the transporters contribute little to cellular Mn levels as majority of the newly synthesized Smf1p and Smf2p polypeptides are degraded in the vacuole (Luk et al., 2003). This constitutive degradation of the transporters supplies the cell with sufficient manganese but minimizes the cellular uptake of toxic metals such as Cd. On the other hand, under Mn starvation conditions, Smf1p and Smf2p abundantly accumulate at the cell surface and intracellular vesicles and are directed away from degradation at the vacuole to increase Mn uptake (Luk et al., 2003).

This shift in localization represents a change in the sorting of Smf1p and Smf2p in the secretory pathway and is mediated by the membrane-bound Bsd2p (*b*ypass *S*OD1 *d*efect; Culotta et al., 2005; Jensen et al., 2009). Under physiological conditions, the majority of Smf1p and Smf2p are conjugated with ubiquitin as they transit the Golgi and marked for vacuolar degradation. Bsd2p is thought to ubiquitin tag misfolded proteins in the secretory pathway and promote their vacuolar degradation (Culotta et al., 2005). Smf1p and Smf2p act as conditional substrates and are recognized by Bsd2p for ubiquitination only under conditions of ample Mn. Bsd2p recruits the E3 ubiquitin ligase Rsp5 to ubiquitinate the transporters and target them to the vacuole (Culotta et al., 2005; Jensen et al., 2014). The interaction between Smf1p/Smf2p and Bsd2p and Rsp5 appears to be linked to Mn concentration in Golgi lumen and it has been proposed that

these transporters can directly sense the Golgi Mn levels (Jensen et al., 2014). However, the precise mechanistic details of how these transporters sense Golgi Mn levels to alter sorting are unknown.

In response to toxic levels of Mn, the yeast cell virtually abolishes uptake of Mn by increasing the vacuolar degradation of Smf1p and Smf2p (Luk et al., 2003). However, an unregulated cell surface phosphate transporter Pho84p, which is a low affinity Mn transporter, continues to pump Mn into the cytosol (Culotta et al., 2005). The accumulated cytosolic manganese is removed by transport into the Golgi through Pmr1p from where it is expelled out of the cell via secretory pathway vesicles. Pmr1p is the prototype of the large family of transporting ATPases known as SPCA (Secretory Pathway Calcium ATPases) found in various fungi, *Caenorhabditis elegans*, *Drosophila melanogaster* and mammals (eg. human SPCA1 and SPCA2; Culotta et al., 2005; Xiang et al., 2005). Yeast cells lacking Pmr1p are extremely sensitive to manganese toxicity and accumulate high concentrations of manganese in the cytosol (Lapinskas et al., 1995). Hence, Pmr1p is not only important for supplying Mn to the Golgi for activation of sugar transferase enzymes but also plays a pivotal role in Mn detoxification.

Thus, in yeast the homeostatic response to increased intracellular Mn accumulation involves change in sorting of proteins involved in Mn uptake into the cell and efflux of excess metal ion via the Golgi.

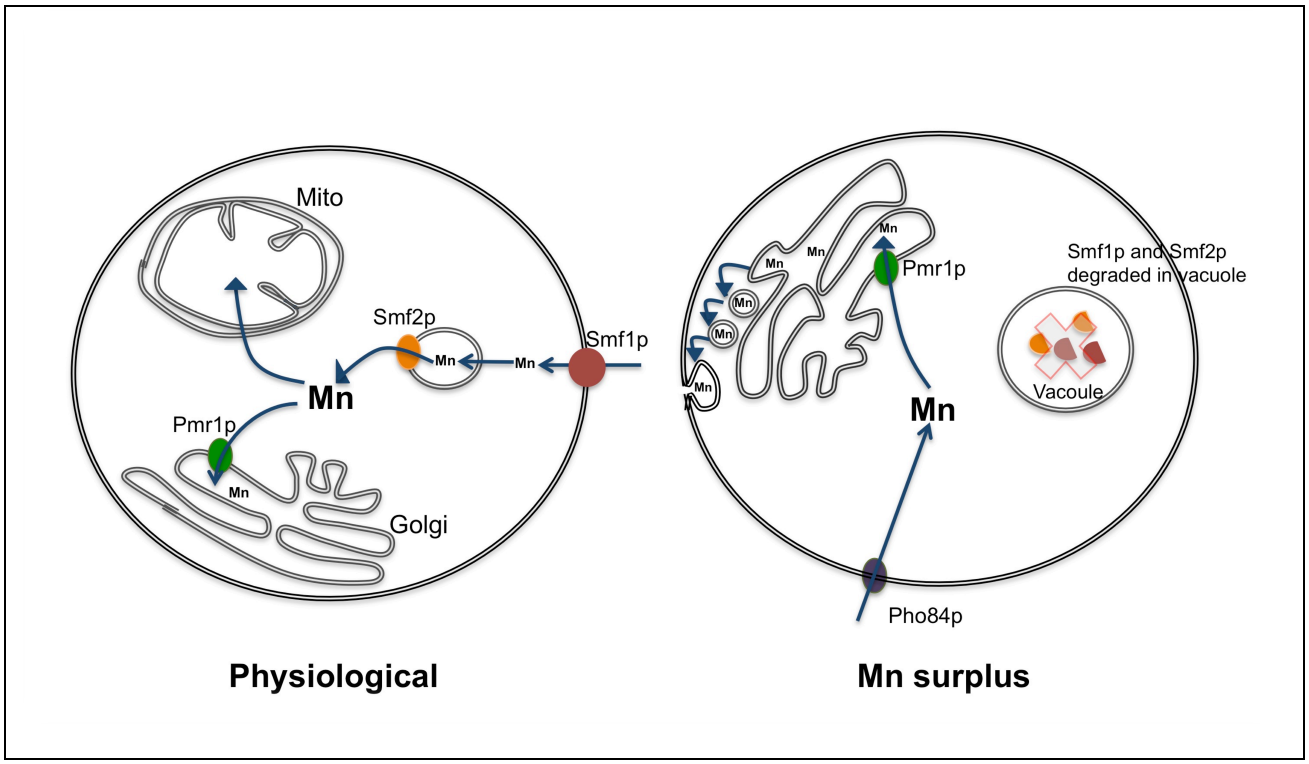

Figure 1-2. Mn uptake and detoxification pathways in *Saccharomyces cerevisiae*.

Under physiological conditions, S. cerevisiae cells uptake Mn via the Nramp metal transporter Smf1p at the cell surface. Mn then traffics through Smf2p-containing vesicles that may represent storage or transient passage stations for the metal. The Smf2p-transported manganese can then move to either the Golgi or mitochondria (mito). Pmr1p pumps Mn into the Golgi for activation of sugar transferase enzymes. On the other hand under conditions of surplus Mn, the metal is taken up largely in the form of Mn-phosphate complexes via the Pho84p phosphate transporter. The excess Mn is then pumped into the Golgi via Pmr1p and it exits the cell via the secretory pathway. (Adapted from Culotta et al., 2005)

Insights into Mn homeostasis in mammalian cells

Taking cues from Mn induced changes in cellular levels of Mn transporters in yeast, studies on Mn homeostasis in mammalian cells have focused on metal influx. These studies have indicated that Mn influx is mediated by a cohort of ion transporters including splice isoforms of the divalent metal transporter 1 (DMT1; Yeast homologue of Smf1p), the solute-carrier 39 metal transporter member ZIP8, transferrin receptor, various calcium channels and glutamate ionotropic receptor (Au et al., 2008). However, these transporters are not specific to Mn and transport other metals cations (Fe, Cd, zinc (Zn)) as well. Further, their cellular localization, levels or transport activities do not appear to be regulated by changes in intracellular levels of Mn (Au et al., 2008), thereby rendering Mn influx unregulated. In contrast, the mechanism of cellular Mn efflux has not been widely studied although metal efflux has been recognized to be an important process mediating homeostasis in metals like Fe, Cu, Zn and Cd (Liuzzi et al., 2004; Troadec et al., 2010; La Fontaine and Mercer, 2007). For instance, as discussed earlier, deficits in metal efflux have been associated with cellular metal accumulation and subsequent toxic effects such as Wilson's disease due to defect in efficient efflux of Cu (Kitzberger et al., 2005; Troadec et al., 2010).

Recently it has been shown that the main route of Mn efflux and detoxification in mammalian cells is via transport of Mn into the Golgi and its subsequent secretion (Mukhopadhyay et al., 2011). The Golgi complex is an integral part of the biosynthetic pathway as it receives newly synthesized proteins from the ER at its *cis*-cisternae and Golgi enzymes mediate post-translational modifications including glycosylation, phosphorylation and sulfation. Once modified, the proteins are next sorted from the TGN

to their target post Golgi compartments. Novel functions of the Golgi have gradually emerged including the aforementioned role in ion homeostasis (La Fontaine and Mercer 2007; Lutsenko et al., 2007; Mukhopadhyay et al., 2011) as well as initiation of several signaling pathways and involvement in cell fate decisions and lipid metabolism (Wilson et al. 2011).

Mn transport into the Golgi in mammalian cells is mediated by a Golgi localized Ca and Mn ATPase pump, SPCA1 (Secretory Pathway Calcium ATPase-1; yeast homologue of Pmr1p; Johaness and Wunder, 2011). Significantly, a mutated version of SPCA1 (Q747A) with heightened Mn pumping activity increases Mn uptake into the Golgi and this promotes Mn efflux by secretion, thereby protecting cells from Mn cytotoxicity (Mukhopadhyay et al., 2011). In other words, increased uptake of Mn into the Golgi leads to lesser Mn accumulation in cells due to its secretion. In contrast, toxicity is exacerbated if Mn transport into the Golgi or Mn secretion is blocked (Mukhopadhyay et al., 2011). Thus, efflux via Golgi is a fundamental homeostatic mechanism that maintains cellular Mn levels and protects against excess Mn accumulation in the cytosol.

1.3 Protein sorting at the Trans Golgi Network

The mammalian Golgi complex is composed of flattened membrane pouches or cisternae aligned in parallel to form a stack (Ladinsky et al. 1999). The Golgi stack is compartmentalized into *cis, medial, and trans* compartments that are enriched with specific Golgi resident enzymes. Secretory pathway proteins transported from the ER enter the stack at the *cis* face, traverse through the various cisternae for post-translational processing and modification and then egress at the *trans* face. The *trans*-most cisterna of the Golgi is continuous with a tubulo-reticular membrane compartment termed the *trans* Golgi network (TGN), which acts as a sorting and distribution center, directing cargo proteins to lysosomes, plasma membrane or the cell exterior for secretion (Bonifacino and Traub, 2003).

It is well established that sorting at the TGN is crucial for the regulation of key cellular events such as polarized distributions of apical and basolateral proteins, metal-ion homeostasis (as discussed above) as well as maintenance of regulated secretion and immunity. Defects in the ability to sort proteins to their appropriate cellular destinations can cause severe pathological conditions. For example, missorting of the basolateral LDLR (Low-Density Lipoprotein Receptor) to the apical surface of hepatocytes leads to accelerated atherosclerosis and an increased risk of premature coronary heart disease (Stein et al., 2002).

Cargo proteins harbor sorting signals for delivery to their respective post-Golgi targets. The resulting pathways of TGN exit include constitutive, regulated, apical-surface, basolateral-surface, early endosome, late endosome, and lysosome, with some of these present only in specialized cells (Polishchuk et al., 2003).

The sorting of proteins from the TGN to the endosomal/lysosomal system has been extensively studied. Classic examples of proteins that follow this route are the newly synthesized lysosomal hydrolases. These bind a transmembrane sorting receptor that interacts with cytosolic adaptors that engage the clathrin vesicle coat complex at the TGN. Two such classes of adaptors are- the Golgi-associated γ-adaptin homologous ARF-interacting proteins or GGA family of monomeric proteins (three members in mammalian cells-GGA1, GGA2 and GGA3) and the heterotetrameric adaptor proteins (APs; Braulke and Bonifacino, 2009). Of the five APs identified in higher eukaryotes, AP-1, AP3 and AP-4 are involved in sorting at the TGN. While GGAs recognize acidic cluster dileucine sorting motifs, APs recognize dileucine and tyrosine based sorting motifs in the cytosolic tails of cargo proteins (Gu et al., 2001).

The TGN membrane localization of GGAs and AP-1 depends on binding to ADP-ribosylation factor (Arf1) and phosphatidylinositol 4-phosphate enriched in TGN membranes (Guo et al, 2014). Polymerization of clathrin along with the associated cargo adaptors forms membrane coat structures. This concentrates the associated cargo molecules into coated membrane microdomains and leads to membrane deformation with the help of coat accessory proteins, ultimately leading to vesicle budding. These vesicles then deliver the cargo to their target destination.

1.4 Golgi glycoprotein GPP130 displays Mn sensitive trafficking

GPP130 is a homodimeric type II single pass transmembrane with a large lumenal domain consisting in part of a predicted coiled-coil domain and an unstructured acidic domain (Linstedt et al., 1997). Under physiological conditions, GPP130 constitutively cycles to maintain its steady state localization in the *cis* cisternae of the Golgi stack. This involves constant trafficking and retrieval from distal compartments such as endosomes (Puri et al., 2002) via the late endosome/lysosome-bypass pathway. In this pathway, GPP130 is retrieved from endosomes by direct trafficking to the Golgi, thereby bypassing the late endosomes and lysosomes. As mentioned, in response to minor increases in intra-Golgi Mn, but not cytosolic, GPP130 redistributes from the Golgi directly to multivesicular bodies in a Rab7 dependent pathway en route to lysosomes for degradation (Mukhopadhyay et al., 2010). This redistribution is insensitive to a dominant negative (DN) version of dynamin, microtubule disruption or DN-Rab5 indicating that neither endocytosis nor early endosome trafficking are involved (Mukhopadhyay et al., 2010). Unlike most other Golgi membrane proteins, the lumenal predicted coiled-coil domain of GPP130 contains distinct Golgi and post-Golgi endosomal targeting determinants that mediate its targeting to the *cis* Golgi, late endosome/lysosome-bypass pathway trafficking (Bachert et al., 2001, Puri et al., 2002) as well as Mn sensitivity (Mukhopadhyay et al., 2010). Although the regular function of GPP130 is uncertain, no other Golgi protein is known to be down-regulated by Mn and Mn is the only divalent ion that affects GPP130 trafficking (Mukhopadhyay et al., 2010).

Mn induced down-regulation of the *cis* Golgi glycoprotein GPP130 thus presents a unique case of metal-regulated protein sorting as well as potential therapy against Shiga toxicosis in mammalian cells. However, the molecular mechanism of the drastic change in sorting of GPP130 in response to increased Golgi Mn is unknown. Does Mn bind GPP130? If so, how does this binding alter sorting of GPP130 to lysosomes and what other factors are involved? These questions are experimentally addressed in chapters 2 and 3. Significantly, the results reveal Mn-induced oligomerization/clustering of GPP130 as the mechanism. Further, they argue that this is a specific case of what appears to be a general pathway in which oligomerized/clustered Golgi proteins are targeted for degradation perhaps as part of quality control.

1.5 REFERENCES

Aschner M., Erikson K.M., Herrero Hernandez E., Hernandez E.H. and Tjalkens R (2009). Manganese and its role in Parkinson's disease: From transport to neuropathology. Neuromolecular Med 11:252-266.

Au, C., Benedetto, A., and Aschner, M. (2008). Manganese in eukaryotes. Neurotoxicology 29, 569–576.

Bachert, C., Lee, T.H., and Linstedt, A.D. (2001) Lumenal endosomal and Golgi‐retrieval determinants involved in pH‐sensitive targeting of an early Golgi protein. Molecular biology of the cell 12(10): 3152‐3160.

Beddoe, T., Paton, A.W., Le Nours, J., Rossjohn, J., and Paton, J.C. (2010). Structure, biological functions and applications of the AB5 toxins. Trends Biochem Sci *35*, 411-418.

Bonifacino, J. S., and Traub, L. M. (2003). Signals for Sorting of Transmembrane Proteins to Endosomes and Lysosomes. Annual review of biochemistry, 72(1), 395-447.

Braulke, T., and Bonifacino, J. S. (2009). Sorting of lysosomal proteins.Biochimica et Biophysica Acta (BBA)-Molecular Cell Research, 1793(4), 605-614.

Burgos, P.V., Mardones, G.A., Rojas, A.L., Luis, L.P., Prabhu, Y., Hurley, J.H., and Bonifacino, J.S. (2010). Sorting of the Alzheimer's Disease Amyloid Precursor Protein Mediated by the AP-4 Complex. Developmental Cell 18, 425–436.

Crossgrove, J. and Zheng, W. (2004). Manganese toxicity upon overexposure. NMR Biomed. 2004;17:544–553.

Culotta, V.C., Yang, M., and Hall, M.D. (2005). Manganese transport and trafficking: lessons learned from Saccharomyces cerevisiae. Eukaryot Cell *4*, 1159-1165.

Durr, G., J. Strayle, R. Plemper, S. Elbs, S. K. Klee, P. Catty, D. H. Wolf, and Rudolph., H.K. (1998). The medial‐Golgi ion pump Pmr1 supplies the yeast secretory pathway with Ca^{2+} and Mn^{2+} required for glycosylation, sorting, and endoplasmic reticulum‐associated protein degradation. Mol Biol Cell 9, 1149‐1162.

Endo, Y., Tsurugi, K., Yutsudo, T., Takeda, Y., Ogasawara, T., and Igarashi, K. (1988). Site of action of a Vero toxin (VT2) from Escherichia coli O157:H7 and of Shiga toxin on eukaryotic ribosomes. RNA N-glycosidase activity of the toxins. Eur J Biochem *171*, 45-50.

Fraser, M.E., Chernaia, M.M., Kozlov, Y.V., and James, M.N. (1994). Crystal structure of the holotoxin from Shigella dysenteriae at 2.5 A resolution. Nat Struct Biol *1*, 59-64.

Gu, F., Crump, C. M., and Thomas, G. (2001). Trans-Golgi network sorting.Cellular and Molecular Life Sciences CMLS, 58(8), 1067-1084.

Guo, Y., Sirkis, D. W., and Schekman, R. (2014). Protein Sorting at the trans-Golgi Network. Annual review of cell and developmental biology, 30, 169-206.

Jensen, L. T., Carroll, M. C., Hall, M. D., Harvey, C. J., Beese, S. E., and Culotta, V. C. (2009). Down-regulation of a manganese transporter in the face of metal toxicity. Molecular biology of the cell, 20(12), 2810-2819.

Jensen, A. N., and Jensen, L. T. (2014). Manganese Transport, Trafficking and Function in Invertebrates. Issues in Toxicology, Chapter 1, Manganese in Health and Disease, pp. 1-*33.*

Johannes, L., and Wunder, C. (2011). Retrograde transport: two (or more) roads diverged in an endosomal tree? Traffic *12*, 956-962.

Kitzberger, R., Madl, C., and Ferenci, P. (2005). Wilson disease. Metab Brain Des 20: 295-302.

La Fontaine, S., and Mercer, J.F. (2007). Trafficking of the copper-ATPases, ATP7A and ATP7B: role in copper homeostasis. Arch Biochem Biophys *463*, 149-167.

Lalioti, V., Muruais, G., Tsuchiya, Y., Pulido, D., and Sandoval, I. V. (2008). Molecular mechanisms of copper homeostasis. Frontiers in bioscience (Landmark edition), 14, 4878-4903.

Lapinskas, P. J., Cunningham, K. W., Liu, X. F., Fink, G. R. and Culotta, V. C.Mutations in PMR1 suppress oxidative damage in yeast cells lacking superoxide dismutase. Mol Cell Biol 15, 1382-1388 (1995).

Linstedt, A.D., Mehta, A., Suhan, J., Reggio, H., and Hauri, H.P. (1997). Sequence and overexpression of GPP130/GIMPc: evidence for saturable pH-sensitive targeting of a type II early Golgi membrane protein. Molecular biology of the cell 8(6): 1073-1087.

Liuzzi, J.P. and Cousins, R.J. (2004). Mammalian zinc transporters. Annu Rev Nutr 24:151-172.

Luk, E., Jensen, T., and Culotta, V. (2003). The many highways for intracellular trafficking of metals. J Biol Inorg Chem 8: 803–809.

Mariko, S., and Jonathan, D. G. (1999). Intracellular localization of the Menkes and Wilson's disease proteins and their role in intracellular copper transport. Pediatrics International 41, 436–442.

Hentze, M.W., Muckenthaler, M.U., and Andrews, N.C. (2004). Balancing Acts: Molecular Control of Mammalian Iron Metabolism. Cell, Vol. 117, 285–297.

Mellman,I and Nelson, W.J. (2008). Coordinated protein sorting, targeting and distribution in polarized cells. Nature Reviews Molecular Cell Biology 9, 833-845.

Mukhopadhyay, S., Bachert, C., Smith, D. R. and Linstedt, A.D. (2010). Manganese induced trafficking and turnover of the cis-Golgi glycoprotein GPP130. Mol Biol Cell 21, 1282-1292.

Mukhopadhyay, S., and Linstedt, A.D. (2011). Identification of a gain-of-function mutation in a Golgi P-type ATPase that enhances Mn2+ efflux and protects against toxicity. Proc Natl Acad Sci U S A 108, 858-863.

Mukhopadhyay, S., and Linstedt, A.D. (2012) Manganese blocks intracellular trafficking of Shiga toxin and protects against Shiga toxicosis. Science 335(6066): 332-335.

Mukhopadhyay, S., and Linstedt, A.D. (2013). Retrograde trafficking of AB(5) toxins: mechanisms to therapeutics. J Mol Med (Berl) 91, 1131-1141.

Olanow, C. W. Manganese-induced parkinsonism and Parkinson's disease (2004). Ann N Y Acad Sci 1012, 209-223.

Reddi, A.R., Jensen, L.T., and Culotta, V.C. (2009). Manganese homeostasis in Saccharomyces cerevisiae. Chem Rev *109*, 4722-4732.

Polishchuk, E.V., Di Pentima, A., Luini, A., and Polishchuk, R.S. (2003). Mechanism of Constitutive Export from the Golgi: bulk flow via the formation, protrusion, and En Bloc Cleavage of large trans-Golgi network tubular domains. Mol. Biol. Cell, 14, pp. 4470–4485.

Polishchuk, R., and Lutsenko, S. (2013). Golgi in copper homeostasis: a view from the membrane trafficking field. Histochem Cell Biol *140*, 285-295.

Puri, S., Bachert, C., Fimmel, C.J., and Linstedt, A.D. (2002). Cycling of early Golgi proteins via the cell surface and endosomes upon lumenal pH disruption. Traffic *3*, 641-653.

Roth, J. A., Horbinski, C., Higgins, D., Lein, P. and Garrick, M. D. (2002). Mechanisms of manganese-induced rat pheochromocytoma (PC12) cell death and cell differentiation. Neurotoxicology 23, 147-157.

Sandvig, K., Bergan, J., Dyve, A.B., Skotland, T., and Torgersen, M.L. (2010). Endocytosis and retrograde transport of Shiga toxin. Toxicon *56*, 1181-1185.

Stein, M.P., Angela W.N., and Roitbak, T. (2002). Altered trafficking and epithelial cell polarity in disease. Trends in cell biology 12.8: 374-381.

Supek, F., L. Supekova, H. Nelson, and N. Nelson (1997). Function of metalion homeostasis in the cell division cycle, mitochondrial protein processing, sensitivity to mycobacterial infection and brain function. J. Exp. Biol. 200: 321–330.

Supek, F., L. Supekova, H. Nelson, and N. Nelson (1996). A yeast manganese transporter related to the macrophage protein involved in conferring resistance to mycobacteria. Proc. Natl. Acad. Sci. USA 93:5105–5110.

Towler, M. C., Prescott, A. R., James, J., Lucocq, J. M., and Ponnambalam, S. (2000). The manganese cation disrupts membrane dynamics along the secretorypathway. Exp. Cell Res. 259, 167–179.

Takeda, A., Sawashita, J., and Okada, S. (1995). Biological half-lives of zinc and manganese in rat brain. Brain Res.695(1): 53–58.

Wilson, C., Venditti, R., Rega, L.R., Colanzi, A., D'Angelo, G., De Matteis, M.A. (2011). The Golgi apparatus: an organelle with multiple complex functions. Biochem J.; 433(1): 1–9.

Xiang, M., D. Mohamalawari, and R. Rao (2005). A novel isoform of the secretory pathway Ca^2-Mn^2-ATPase, hSPCA2, has unusual properties and is expressed in the brain. J. Biol. Chem. 280:11608–11614.

CHAPTER 2

Manganese Induces Oligomerization to Promote Down-regulation of GPP130- the Intracellular Trafficking Receptor used by Shiga Toxin

2.1 ABSTRACT

Manganese (Mn) protects cells against lethal doses of purified Shiga toxin by causing the degradation of the cycling transmembrane protein GPP130, which the toxin uses as a critical trafficking receptor. Mn-induced GPP130 down-regulation, in addition to being a potential therapeutic approach against Shiga toxicosis, is a model for the study of metal-regulated protein sorting. Significantly, however, the mechanism by which Mn regulates GPP130 trafficking is unknown. Here we address whether GPP130 binds Mn and, if so, how Mn binding alters GPP130 trafficking to cause GPP130 degradation. To this end, we mapped a transferable sequence element of about 50 residues in the lumenal stem domain of GPP130 that confers Mn sensitivity and observed that alanine substitutions within this element abolished Mn-sensitive trafficking. Significantly, a purified version of the determinant bound Mn and Mn binding induced its oligomerization, whereas the same alanine substitutions blocked both activities. Further, Mn treatment of cells caused a dramatic increase in the apparent size of wildtype GPP130 in the Golgi, but not the alanine substituted variant. Remarkably, oligomerization was sufficient because GPP130 was redirected to lysosomes in the absence of Mn by forced aggregation using a drug-controlled polymerization domain. These experiments reveal metal-induced oligomerization as a Golgi sorting mechanism for a medically relevant receptor for Shiga toxin.

2.2 INTRODUCTION

Shiga, cholera and pertussis toxins belong to the notorious class of AB_5 bacterial toxins consisting of catalytic A subunits carried into cells by their associated homopentameric B subunits (Sandvig *et al.*, 2010). These toxins invade host cells by a retrograde route involving endocytosis, transport via the Golgi to the ER and translocation of the A subunit out of the ER to the cytoplasm (Mallard and Johannes, 2003). In the case of Shiga toxin, the A subunit causes cytotoxicity by inactivating ribosomes to shut down host cell protein synthesis (Endo *et al.*, 1988) (Fraser *et al.*, 1994). Shiga infections involve life-threatening diarrhea, dysentery, and hemorrhagic colitis, all of which can lead to fatal hemorrhagic uremic syndrome (Beddoe *et al.*, 2010). Treatment options, mostly involving hydration, are extremely limited and indirect.

As it invades host cells, Shiga toxin avoids degradation in lysosomes by sorting into endosomal membrane tubules that move directly to the Golgi (Johannes and Wunder, 2011). For two major isoforms of Shiga toxin, STx (present in Shigella) and STx1 (present in strains of E. coli), sorting into endosomal tubules is mediated by their binding to GPP130, a host cell transmembrane protein that constitutively cycles between endosomes and the Golgi (Mukhopadhyay and Linstedt, 2012). A binding site on the outside sidewall of the doughnut shaped toxin B subunit engages a site near the membrane of the lumenal stem domain of GPP130, which is predicted to form a homodimeric coiled-coil (Mukhopadhyay *et al.*, 2013). In this way it is thought that STx/STx1 piggybacks a ride to the Golgi.

Therapeutic approaches that block toxin sorting in endosomes serve the dual

purposes of blocking toxin movement to the Golgi and diverting it to lysosomes where it is degraded and cleared from infected cells (Mukhopadhyay and Linstedt, 2013). Thus, it is serendipitous that a relatively moderate increase in extracellular manganese (Mn) down-regulates GPP130 levels (Mukhopadhyay *et al.*, 2010). Indeed, non-toxic doses of Mn block STx/STx1 trafficking to the Golgi, cause toxin degradation in lysosomes, and prevent fatal toxicosis in both cultured-cell and mouse models (Mukhopadhyay and Linstedt, 2012).

GPP130 down-regulation by elevated extracellular Mn involves Rab7-dependent movement of GPP130 from the Golgi to multivesicular bodies (MVB) and lysosomes and this response requires the Golgi-localized Ca2+/Mn2+ pump indicating that it is increased Mn in the Golgi which alters GPP130 sorting out of the trans Golgi network (TGN) (Mukhopadhyay *et al.*, 2010). Although GPP130 is a unique example of Mn-sensitive trafficking in mammalian cells, there are important examples of altered membrane protein sorting by metal ions, particularly in relation to regulating ion homeostasis. Elevated copper causes the reversible redistribution of two copper transporters, ATP7A and ATP7B, from the TGN to the plasma membrane to expel copper and protect against its toxicity (La Fontaine and Mercer, 2007). Blocking mutations of the transporters have been identified but the relevant target of copper and how it alters transporter TGN export remain unknown (Polishchuk and Lutsenko, 2013). Another example is provided by manganese homeostasis in Saccharomyces cerevisiae, which is controlled, in part, by trafficking of the Smf1p and Smf2p transporters (Reddi *et al.*, 2009). In the absence of Mn, the transporters traffic through the secretory

pathway to the cell surface to scavenge any available ion. As manganese levels rise, the proteins are instead diverted to vacuoles where they are degraded. Significant progress has been made on the mechanism of Smf1p/2p targeting to intraluminal vesicles of the MVB by ubiquitination (Sullivan *et al.*, 2007; Jensen *et al.*, 2009) but, again, the relevant target of the metal and how it alters TGN sorting is unknown.

Thus, while metal-induced changes in membrane trafficking are an important theme in ion homeostasis there is a strong need for understanding the key step in which the metal is sensed causing a change in sorting. To bind at low metal concentrations, constitutively occupied metalloproteins utilize high affinity sites involving an array coordinating charged side chains (Borgstahl *et al.*, 1992). In contrast, a protein that binds and responds to elevated metal concentrations might exhibit weaker affinity perhaps by only partially coordinating the ion. Given the importance of identifying a metalloprotein undergoing metal-regulated sorting, we sought to determine whether Mn binds GPP130 and, if so, how it might alter GPP130 sorting. Our results indicate that GPP130 does interact directly with Mn and this interaction causes a dramatic change in its assembly state both in vitro and in living cells. Further, this is required and sufficient to down-regulate the protein.

2.3 RESULTS

Mn-sensitive determinant

Our previous work showed that the GPP130 lumenal stem domain conferred Mn-sensitive targeting when appended to GP73, a structurally similar cis Golgi protein whose trafficking is otherwise not altered by Mn (Mukhopadhyay et al., 2010). Within the lumenal stem domain the juxta-membrane residues 36-175 were clearly important and became our focus in the present study. To further map residues conferring Mn sensitivity, a series of GPP130 sequence segments from this region were positioned between the GP73 N-terminus (containing cytoplasmic, transmembrane and stem domain) and GFP and the chimeric proteins were expressed in HeLa cells. Mn sensitivity was measured by the ability of the transfected constructs to begin redistributing to endosomal structures in response to a 2 h exposure to a nontoxic dose of 500 μM $MnCl_2$. This time point is before substantial degradation occurs and leaves a large amount of GPP130 in the Golgi aiding the identification and quantification of the transfected cells. For presentation, saturated images are used because GPP130 redistributes to MVB/lysosomes where it is degraded relatively rapidly (Mukhopadhyay et al., 2010). For quantification, unaltered images captured at equivalent exposures were processed to determine the number of non-Golgi puncta in the presence or absence of Mn. A pretreatment of cycloheximide for 2 h was used to prevent overexpression and deplete any ER pool of protein. Endogenous GPP130, detected with a non-crossreacting antibody was used to confirm an intact Mn response in the same cells.

Figure 1 shows the localization of a few key constructs before and after Mn (Fig 2-1A) as well as schematic depictions of the tested GPP130 segments together with their corresponding quantified presence in peripheral puncta (Fig 2-1B). Consistent with our previous work (Mukhopadhyay et al., 2010), residues 36-175 produced a strong response shifting from fewer than 5 non-Golgi puncta per cell in the absence of Mn to over 30 puncta per cell in the presence of Mn. As noted before (Mukhopadhyay et al., 2010), most of the puncta contained redistributed endogenous GPP130, whereas not all endogenous GPP130 puncta were positive for the transfected construct. Deletions in from the C-terminal side generated constructs 36-107, 36-100, 36-95, and 36-87. All of these except 36-87 retained activity indicating that residues 88-95 were critical. A similar set of truncations to winnow in from the N-terminal side indicated that the first 13 residues (36-49) were dispensable with larger deletions causing loss of activity. This left 50-100 as the smallest active construct and the sequence stretch 88-95 as a tractable segment for point mutation. Several individual and combined alanine substitutions within 88-95 were without effect but alanine substitution of the sequence $_{88}$DFLV$_{91}$ to generate 36-95-$_{88}$AAAA$_{91}$ potently blocked activity. The non-responsive construct was stable and well localized and did not prevent the endogenous GPP130 response in the same cells. Insertion of the quadruple alanine substitution into the original construct to generate 36-175-$_{88}$AAAA$_{91}$ also strongly blocked its response. In summary, our mapping studies narrowed a transferable Mn responsive sequence to about 50 residues and, more

importantly, identified a required sequence stretch that when mutated could be used as a critical negative control in subsequent experiments.

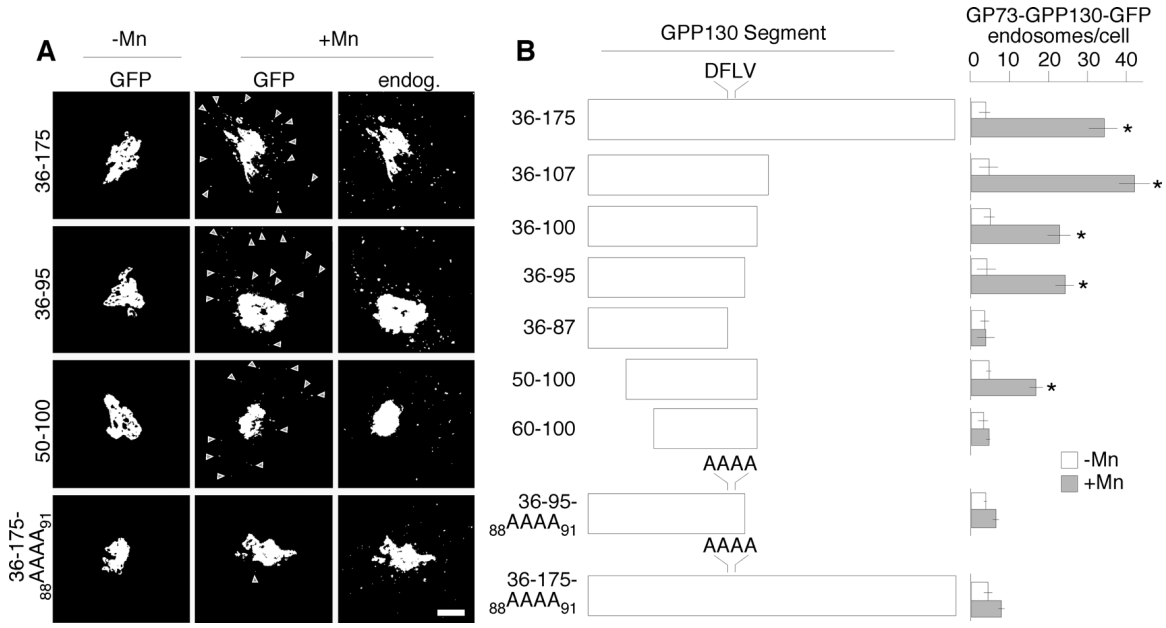

Figure 2-1. GPP130 lumenal sequence element confers Mn sensitivity.

(A) Localization is shown for GFP-tagged GP73 constructs containing the indicated GPP130 residues in the absence or presence of 0.5 mM $MnCl_2$ for 2 h. The images are cropped and identically thresholded to accentuate presence in peripheral punctae. Arrowheads indicate positions of example punctae. The localization of endogenous GPP130 in the same Mn-treated cells serves as an internal control for the Mn response. The chimeric constructs contain the cytoplasmic, transmembrane and stem domain of GP73 followed by a GPP130 segment followed by GFP. Prior to analysis the cells were treated with 0.1mg/ml cycloheximide for 2 h to prevent new synthesis. Size bar = 2 μm.

(B) Schematic diagram of the GPP130 segments present in the GFP-tagged GP73 chimeric constructs and the quantified determination of their presence in peripheral endosomal structures in the absence or presence of Mn. Object analysis is described in Methods. Values are averages (n>25 cells, ±SEM).

Mn induced a statistically significant increase in GFP endosomes per cell in GP73-GPP130 $_{36\text{-}175}$-GFP, GP73-GPP130$_{36\text{-}95}$-GFP, GP73-GPP130$_{50\text{-}100}$-GFP (mean ± SEM, n> 25 cells for each construct with and without Mn; $p < 0.05$) but not in GP73-GPP130$_{36\text{-}175\text{-}88\text{-}AAAA\text{-}91}$-GFP ($p > 0.05$).

Mn binding and oligomerization

Based on the transferability of the Mn response it seemed possible that the GPP130 stem domain might bind Mn. As a test, uncoated or Mn-coated NTA-agarose beads were incubated with the purified GST-tagged GPP130 residues 36-247 and recovery after washing was determined by SDS-PAGE and Coomassie staining. As control proteins we used GST itself and GST fused to the stem domain of GP73. The control proteins showed low recovery on the beads, whereas the GST-tagged GPP130 stem domain (36-175) appeared to interact strongly and specifically with the Mn-coated beads (Fig 2-2A). To estimate the Mn concentration required for half-maximal binding, the experiment was repeated by adding the GPP130 protein (36-247) to increasing concentrations of Mn and then recovering any formed complexes using uncoated NTA-agarose beads. Under these conditions 0.4 mM Mn yielded half-maximal binding (Fig 2-2B). The concentration of Golgi Mn in Mn-treated cells is unknown but the GPP130 response is observed at concentrations of extracellular Mn as low as 0.2 to 0.5 mM, thus it seems reasonable that binding of Mn by the GPP130 stem domain takes place during the GPP130 response. Based on these results we next compared the Mn binding of the GPP130 stem domain to two non-responsive GPP130 constructs. The mapping described above indicated that residues comprising an N-terminal segment of the stem domain (36-87)

contribute to the Mn-response but, on their own, they are not sufficient. Also, alanine substitution of residues 88-91 in the stem domain blocked the Mn response. Therefore, we purified GST-tagged 36-87 and 36-175-$_{88}$AAAA$_{91}$ and compared the binding of these proteins to uncoated and Mn-coated beads with that of a wildtype 36-175 construct. Each construct showed some recovery on Mn-coated beads but the binding was significantly higher for the wildtype construct (Fig 2-2C). Thus, maximal Mn binding in the assay required the same residues that are required for Mn-responsiveness.

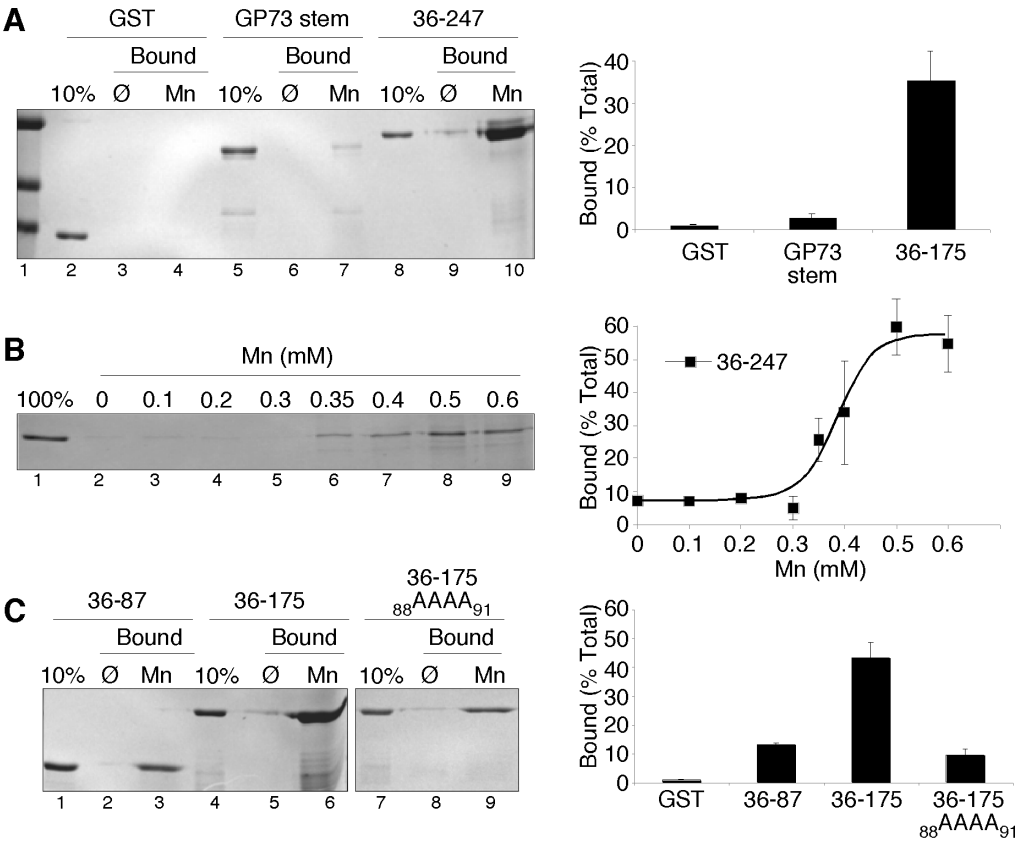

Figure 2-2. Mn binding by the GPP130 stem domain.

(A) Recovery of purified GST, GST-tagged stem domain of GP73, or GST-tagged residues 36-247 of GPP130 on either uncoated or Mn-coated agarose beads. The Coomassie stained gel

also shows 10% of the total of each protein used in the binding assay. Quantification indicates the percent bound to Mn-coated beads for each protein (n=3, ±SEM) * denotes $p<0.01$ or 35.5% ± 6.9% of the GST-GPP130$_{36-247}$ load bound Mn- coated agarose beads, which was significantly different ($p<0.01$) from the negligible binding by GST and GST-GP73$_{36-195}$. There was no significant binding to NTA-agarose beads.

(B) Coomassie stained gel and quantification indicating recovery of GST-tagged residues 36-247 of GPP130 after incubation with beads at the indicated concentrations of $MnCl_2$ (n=3, ±SEM).

(C) Recovery on uncoated or Mn-coated beads of purified GST-tagged GPP130 residues 36-87, 36-175, or 36-175 with the $_{88}AAAA_{91}$ substitution. Quantification of the Coomassie stained gels is also shown for Mn-coated beads (n=3, ±SEM, $p< 0.05$).

Interestingly, the purified GPP130 stem domain constructs 36-247 and 36-175 appeared to oligomerize in response to Mn addition. For example, in the absence of added Mn, GST-GPP130 36-247 was recovered roughly in the middle of velocity gradients, whereas addition of 1 mM $MnCl_2$ shifted most of the protein towards the bottom of the gradients (Fig 2-3A). Mn-induced aggregation of the protein was also apparent simply by measuring absorbance at 350 nm indicating light scattering. Whereas the two purified control proteins, GST and GST-tagged GP73 stem failed to show an increase, the GST-GPP130 36-247 protein yielded a robust increase clearly evident at 1.0 mM $MnCl_2$ (Fig 2-3B). This effect was reversible because it was abrogated by a subsequent incubation with equimolar EDTA to chelate the Mn (Fig 2-3C). Importantly, the alanine substitutions that blocked GPP130 responsiveness in cells and reduced binding of Mn in the GST-GPP130 stem construct (36-175$_{88}AAAA_{91}$) also reduced the Mn-induced light scattering activity of this construct (Fig 2-3D). These results

suggest that Mn binding might promote altered GPP130 trafficking by binding and inducing GPP130 oligomerization.

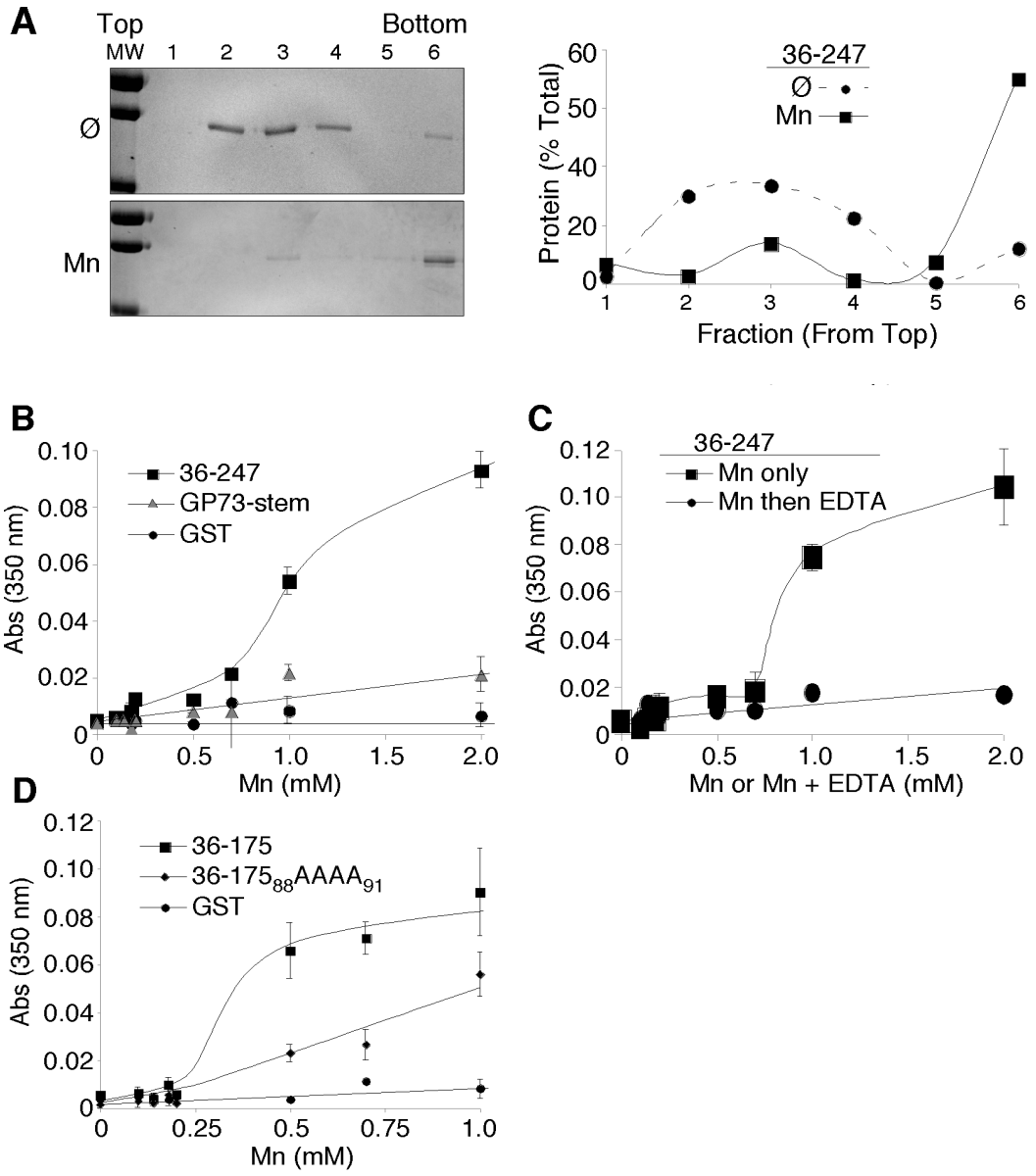

Figure 2-3. Oligomerization of the purified lumenal stem domain.

(A) Coomassie stained gel and quantification indicating recovery of purified GST-tagged residues 36-247 after velocity gradient centrifugation in the absence or presence of 1 mM $MnCl_2$. Result shown is representative of three independent trials.

(B) Light-scattering as indicated by absorbance at 350 nm at the indicated concentrations of $MnCl_2$ for purified GST-tagged residues 36-247 of GPP130, GST-tagged GP73 stem domain, or GST alone (n=5, ±SEM).

(C) Light-scattering after incubation at the indicated concentrations of $MnCl_2$ for 10 min followed by incubation for another 10 min with either no addition or addition of equimolar EDTA to chelate and reverse the effect of Mn binding (n=3, ±SEM).

(D) Light-scattering for purified GST-tagged 36-175, 36-175 with the $_{88}AAAA_{91}$ substitution, and GST alone (n=3, ±SEM).

Mn-induced oligomerization and trafficking

To test the hypothesis that Mn-induced oligomerization alters GPP130 trafficking, we first carried out crosslinking of untreated and Mn treated cells using the membrane permeant crosslinker DSP. A 3 h Mn treatment was used to initiate GPP130 redistribution while leaving a substantial Golgi-localized pool. After cell lysis, the sedimentation behavior of endogenous GPP130 was determined on velocity gradients. In the absence of Mn, GPP130 was recovered near the top of the gradients, whereas Mn treatment resulted in recovery of almost 20% of the GPP130 in a much larger species near the bottom of the gradients (Fig 2-4A). Note that Mn was removed at the time of crosslinking and was absent for the remainder of the experiment, so the change in GPP130 behavior occurred in the intact cells. Also, even in the absence of crosslinking, there was a reproducible, albeit small, fraction of GPP130 in the bottom fractions of lysates from Mn-treated cells but not control cells (not shown). As a negative control, we also examined the behavior of endogenous GP73, which was recovered at the top of the gradients for both untreated and Mn treated cells (Fig

2-4B). One concern was that the Mn-induced oligomerization of GPP130 might not be restricted to the Golgi. As a test we carried out the crosslinking experiment on cells treated with Mn at 20°C to prevent GPP130 exit from the TGN. Immunofluorescence was used to confirm that 20°C incubation blocked redistribution of GPP130 into endosomes (not shown). Under these conditions, GPP130 was still recovered in the size-shifted fractions indicating that oligomerization occurred in the Golgi (Fig 2-4C). Finally, we compared the oligomerization activity of the Mn-responsive wildtype GPP130 stem domain construct described above (Fig 2-1, residues 36-175 of GPP130 appended to the GP73 N-terminus) to the identically constructed protein containing the alanine substitutions that prevent Mn-induced trafficking to lysosomes ($36\text{-}175_{88}AAAA_{91}$). Whereas the 36-175 construct was partly recovered as a much larger species, the alanine substituted construct was recovered exclusively in the top fractions of the gradients (Fig 2-4D).

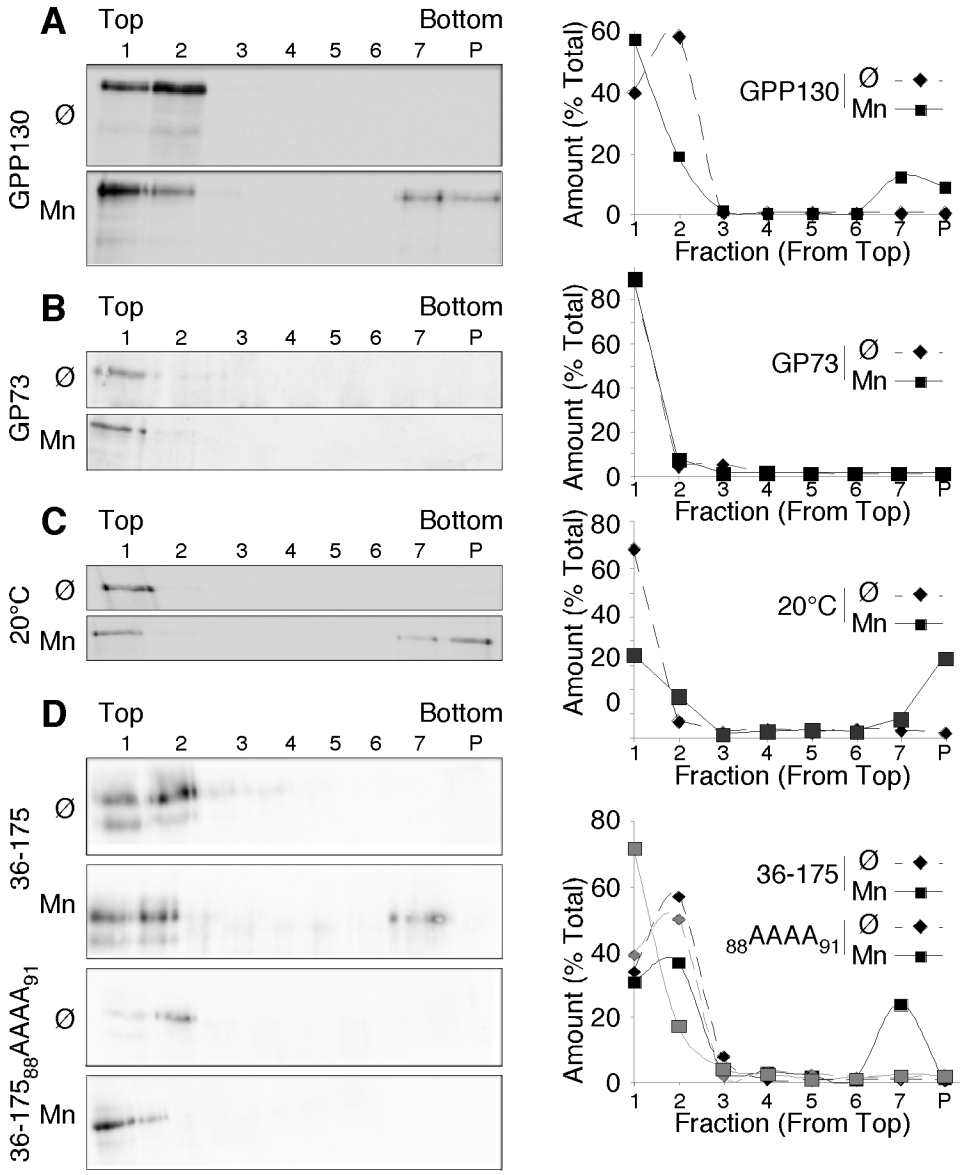

Figure 2-4. Mn-induced oligomerization of Golgi GPP130.

(A) Immunoblots using anti-GPP130 antibodies to detect endogenous GPP130 after velocity gradient fractionation of detergent solubilized cell lysates. Cells were either untreated (Ø) or treated with 0.5 mM $MnCl_2$ for 3 h (Mn) followed by crosslinking with 0.5 mM DSP. The quantified distribution profile is also shown. The entirety of each fraction was analyzed including the resuspended pellet (P). Gradients did not contain Mn. Results are representative of three trials.

(B) Immunoblot and quantified profile using anti-GP73 to detect endogenous GP73 in an identical experiment. Results are representative of three trials.

(C) Immunoblot to detect endogenous GPP130 in and identical experiment except that the 3 h incubation (with or without Mn) was carried out at 20°C to arrest GPP130 in the TGN. Results are representative of three trials.

(D) Immunoblot detection of transfected GP73 chimeric constructs containing GPP130 residues 36-175 without or with the $_{88}AAAA_{91}$ substitution. Exactly as before, the cells were untreated or Mn-treated, subjected to crosslinking, lysed and fractionated on velocity gradients. The quantified fractionation profiles are also shown. Results are representative of three trials.

Next, we used fluorescence recovery after photobleaching to assess whether we could visualize an Mn-induced change in GPP130 diffusion in the Golgi. Cells were first transfected with a GFP-tagged GPP130 construct comprising the cytoplasmic, transmembrane, and stem domains and then were either untreated or treated with Mn. The Mn exposure was for 1 h to initiate GPP130 redistribution but leave a substantial Golgi pool for analysis. A small region of this Golgi fluorescence was bleached and recovery was determined over the next 10 min. Remarkably, the rapid recovery of GPP130 fluorescence in the Golgi of untreated control cells was significantly delayed in Mn treated cells (Fig 2-5A). Quantification of fluorescence recovery in multiple independent trials confirmed that Mn induced a significant delay in GPP130 diffusion (Fig 2-5B). Note that in all other aspects the Golgi fluorescence patterns of treated and untreated cells appeared indistinguishable. To test whether the blocking alanine substitutions would also prevent this Mn-induced delay in recovery, the experiments were repeated with the wildtype and alanine substituted GP73-GPP130 chimeric constructs containing the GPP130 segment 36-175 followed by

GFP. As expected, the wildtype construct rapidly recovered from photobleaching in the absence of Mn and showed a strong delay in recovery in Mn treated cells (Fig 2-5C). In striking contrast, the $_{88}$AAAA$_{91}$ substitution completely abrogated the Mn-induced delay in diffusion such that both untreated and treated cells exhibited identical recoveries (Fig 2-5D). The final extent of recovery for the alanine substitution also matched that of the wildtype construct in untreated cells. For an unknown reason the extent of recovery of these chimeric constructs was lower than that observed for the GPP130 construct. Thus, in living cells, Mn induces a change in GPP130 diffusion in the Golgi that depends on the same residues implicated in Mn binding and Mn-induced oligomerization.

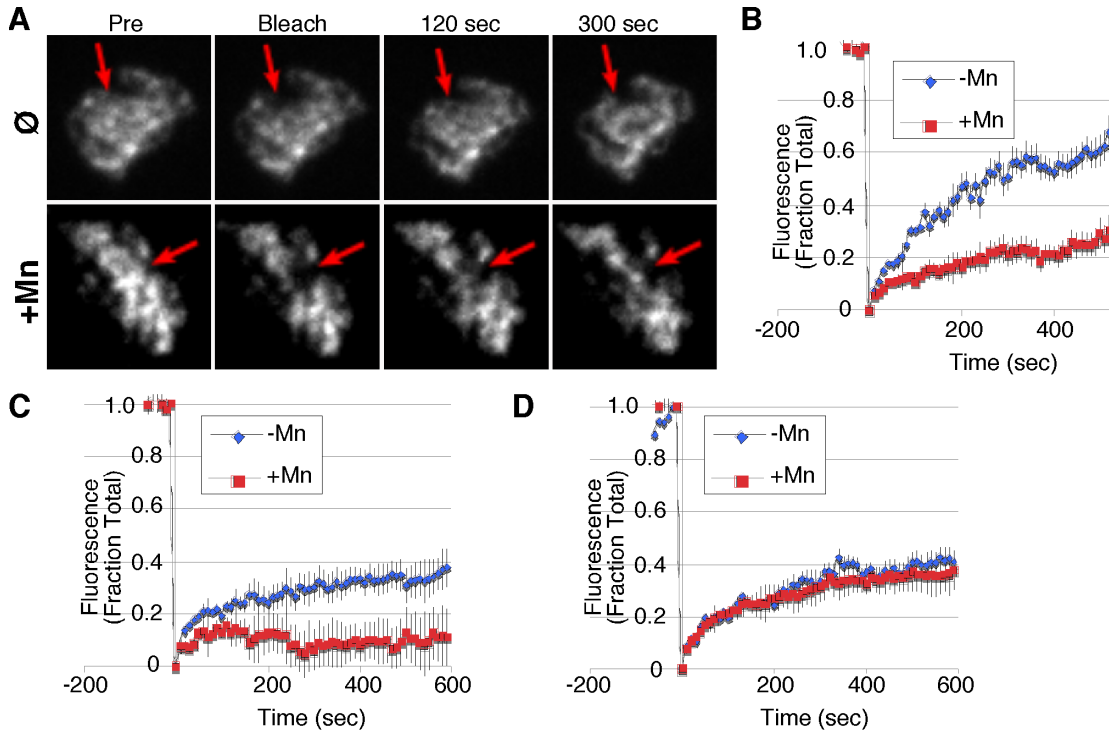

Figure 2-5. Mn slows diffusion of GPP130 in the Golgi.

(A) Fluorescent images of GPP130 tagged with GFP in untreated or Mn-treated cells immediately before a small zone of the Golgi was bleached (arrow) and 0, 2 and 5 min after the bleaching.

(B) Quantified fluorescence levels of GPP130-GFP in the bleached zone at time points before and after bleaching for untreated and Mn-treated cells (n≥10, ±SEM).

(C) Quantified fluorescence levels of the chimeric GP73-GPP130 construct containing the wildtype GPP130 segment 36-175 in the bleached zone at time points before and after bleaching for untreated and Mn-treated cells (n≥10, ±SEM).

(D) Quantified fluorescence levels of the chimeric GP73-GPP130 construct containing the $_{88}$AAAA$_{91}$ substitution in the GPP130 segment 36-175 in the bleached zone at time points before and after bleaching for untreated and Mn-treated cells (n≥10, ±SEM).

Oligomerization induces sorting to lysosomes

Because Mn alters GPP130 oligomerization status in the Golgi contemporaneous with Mn-induced movement of GPP130 to lysosomes we next tested whether oligomerization is sufficient to cause sorting of GPP130 to lysosomes. Versions of GPP130 were constructed harboring the FM oligomerization domain (Rizzo et al., 2013). This segment contains 3 copies of a self-interacting motif that can be controlled by an analog of rapamycin. In the presence of the drug, self-interactions of the FM domains are inhibited and, in the case of the GPP130 construct, the protein yields a stable localization in the Golgi (Fig 2-6A). Significantly, however, upon drug washout the GPP130 construct redistributed to endosome-like peripheral punctae and then disappeared altogether. As a control, giantin in the same cells remained Golgi localized throughout. The redistribution occurred rapidly (Fig 2-6B) with degradation nearing completion by 4 h (Fig 2-6C). Thus, induced oligomerization of GPP130 is sufficient to alter its sorting such that it traffics out of the Golgi and is degraded.

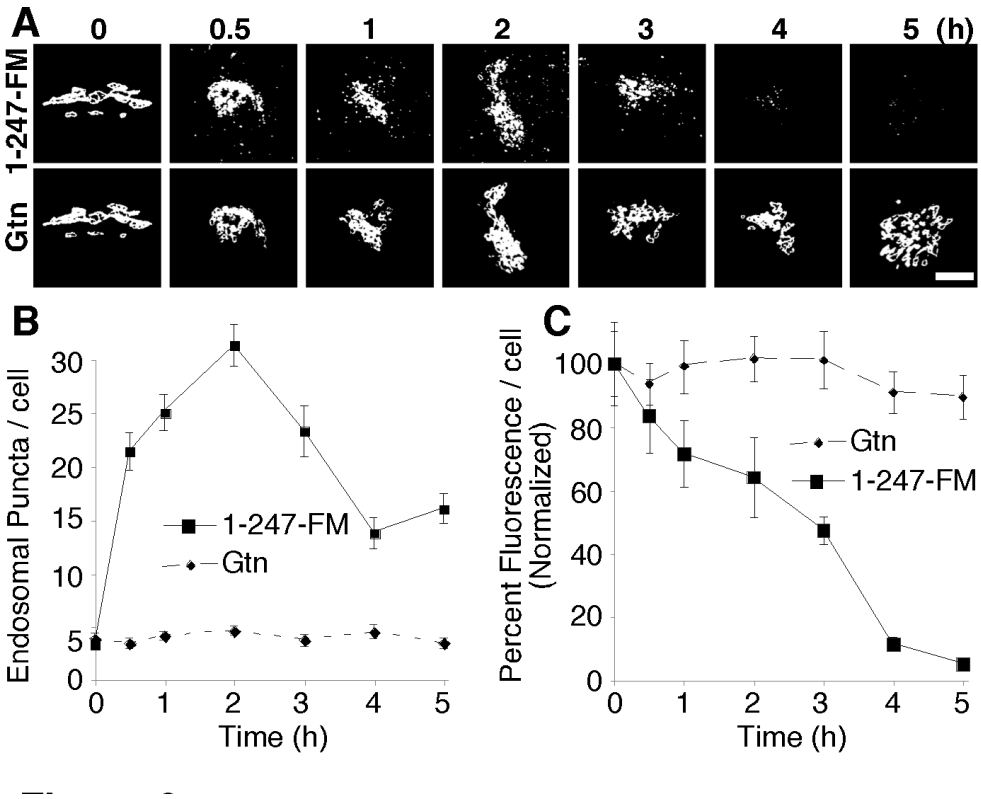

Figure 2-6. Forced GPP130 oligomerization causes loss of Golgi localization and degradation.

(A) Fluorescent images of GPP130 tagged with the FM oligomerization domain (1-247-FM) in cells at the indicated times after AP washout to induce oligomerization. The Golgi marker giantin (Gtn) is shown in the same cells. Bar=2μm.

(B) Quantified number of fluorescent puncta per cell for 1-247-FM and giantin at various times of AP washout (n=3, ±SEM).

(C) Quantified total fluorescence signal per cell for 1-247-FM and giantin at various times of AP washout (n=3, ±SEM).

2.4 DISCUSSION

Mn-induced GPP130 down-regulation provides an avenue to protect cells against fatal invasion by Shiga toxin. Here we asked whether GPP130 down-regulation involves Mn binding to GPP130. This seemed possible because GPP130 down-regulation requires elevated Mn inside the Golgi and involves a lumenal GPP130 sequence element that is transferrable. Indeed, a purified version of this sequence element bound Mn and mutations that blocked binding also blocked GPP130 down-regulation. Significantly, the mechanism of Mn-regulated sorting appeared to involve Mn-induced GPP130 oligomerization because: Mn caused oligomerization of the purified GPP130 sequence element, Mn treatment of cells increased sedimentation of GPP130 on velocity gradients, and Mn reduced GPP130 diffusion in Golgi membranes of living cells. Each of these Mn-induced changes was blocked by alanine substitutions that interfered with Mn binding to GPP130. Further, appending an AP-regulated oligomerization motif to GPP130 yielded an independent demonstration of oligomerization-induced GPP130 down-regulation. Maturation, which is a prevailing model for membrane flux in the Golgi (Emr *et al.*, 2009), stipulates that localization of Golgi residents depends on their capture by small retrieval vesicles. Oligomerization could interfere with this process causing progression of the oligomerized complex together with the membranes of the maturing cisternae. This would move GPP130 to the TGN where, under these conditions, it is then directed towards lysosomes, perhaps by default. Thus, by this view, Mn controls GPP130 down-regulation by regulating its access to cisternal maturation.

A detailed description of Mn binding by the GPP130 stem domain is an important future direction. While atypical, metallo-coiled-coil complexes can be formed (Chakraborty et al., 2010; Berwick et al., 2014). It will be significant to see if Mn binding by GPP130 shares any features with these or other metal binding proteins. Currently, the stoichiometry of Mn binding to GPP130 is unknown and the DFLV sequence we mutated provides little clue regarding the nature of the interaction. Binding of Mn by GPP130 is relatively weak taking place above 100 μM. Although the concentration range of free Mn in the Golgi is unknown, it seems reasonable that upon Mn exposures such as those in our experiments, Golgi Mn rises above 100 μM. Golgi enzymes that use Mn as a cofactor bind Mn with relatively high affinity and are presumably metal bound under normal conditions. In contrast, under these conditions GPP130 remains Golgi localized implying it has a lower affinity Mn interaction. Whereas high affinity sites typically involve full coordination of their bound metal ions, an interesting implication of a low affinity interaction is that it may be achieved by an individual GPP130 dimer only partially coordinating its bound Mn ion. This possibility is consistent with the observation that GPP130 readily binds Mn that is already bound to NTA (Fig2) and it also suggests a possible mechanism of Mn-induced oligomerization. That is, inside the Golgi, single Mn ions may simultaneously bind and link distinct GPP130 coiled-coils thereby becoming fully coordinated and in the process clustering GPP130 dimers into large complexes in the membrane.

Many studies have hinted at a functional link between aggregation and sorting. Aggregation could concentrate proteins into microdomains and also

increase the ratio of sorted protein to sorting receptor. One example is regulated secretion in endocrine cells where peptide hormones form para-crystalline arrays that are packaged into dense core granules (Freedman and Scheele, 1993; Shennan et al., 1994; Colomer et al., 1996). Granule formation is initiated in the TGN, the likely location of sorting of Mn-induced GPP130 oligomers towards lysosomes, raising the question of how GPP130 behaves in response to Mn in endocrine cells. It is important to note that while purified GPP130 can homo-oligomerize (Fig2-3), the GPP130 complexes that form in cells may or may not include other proteins. Another example is oligomerization-dependent apical sorting. The neurotrophin receptor p75 requires transmembrane residues for dimerization and higher-order oligomer formation and mutation of these sites prevents its apical sorting (Youker et al., 2013). Perhaps the most relevant example of aggregation-induced sorting is that reported for the protein convertase furin, which resides in the TGN. Furin is activated by its own processing in the TGN (Anderson et al., 1997). The resulting product is somewhat prone to aggregation and conditions that accelerate its aggregation cause its degradation in lysosomes. Intriguingly, it is thought that the furin stem domain is critical to this sorting behavior. Whether or not this and the Mn-induced change in GPP130 sorting are part of a quality control pathway in which aggregated proteins in the Golgi are targeted for degradation is a significant question.

How might GPP130 oligomers be directed towards lysosomes while the normal dimeric protein undergoes endosome cycling and retrieval? As mentioned

above, the first step might be steric constraints that prevent large protein complexes from accessing small vesicles. If most paths out of the TGN involve sterically restricted sorting, this would leave Mn-bound GPP130 few options for exit from the TGN. Perhaps, there is a type of default for such complexes in which the membranes acquire targeting machinery for traffic towards lysosomes. Alternatively, GPP130 oligomer formation may unmask or generate a targeting signal that promotes its active sorting into a lysosome-directed pathway. It will be important to determine the sorting factors involved on both sides of the membrane. To date it is known that Rab7 is required and that if ubiquitination is involved it must occur on some other protein because the GPP130 cytoplasmic domain is not required (Mukhopadhyay et al., 2010). A final possibility is that GPP130 oligomerization directly alters partitioning of the protein in the TGN, perhaps via lipid interactions, so that it gains access to the lysosome pathway. The observation that Mn-induced GPP130 degradation maps to the stem domain rather than the transmembrane domain argues against this possibility.

The function of GPP130 remains unknown but few, if any, other proteins are down-regulated by Mn and Mn is the only divalent ion that causes this effect (Mukhopadhyay et al., 2010). On this basis, our working hypothesis is that GPP130 is involved in Mn homeostasis. For example, it could be a negative regulator of components involved in reducing cytoplasmic Mn. One mechanism of Mn control involves its sequestration in the Golgi followed by secretion (Culotta et al., 2005; Mukhopadhyay and Linstedt, 2011). When extracellular Mn is low, activities such as SPCA1-mediated movement of Mn into the Golgi may be

dampened to maintain basal levels of Mn in the cytoplasm. Upon increased Mn load, these activities might be upregulated to protect again toxic cytoplasmic concentrations. Thus, when Mn reaches a high-level in the Golgi it binds GPP130 causing GPP130 down-regulation, which in turn, would accelerate Mn sequestration and secretion. So far, GPP130 has not been shown to interact with SPCA1 or other Golgi components.

In closing, the purpose of Mn-induced GPP130 degradation remains a future direction but because GPP130 is used by Shiga toxin to invade cells, Mn-induced GPP130 degradation presents itself as a possible inexpensive and readily available therapy for a devastating disease. Mn-induced GPP130 degradation also provides a paradigm for regulation of membrane trafficking. Our results indicate that GPP130 contains a coiled-coil Mn-binding domain that senses elevated concentrations of Mn in the Golgi lumen. Upon Mn binding, GPP130 undergoes oligomerization and this is necessary and sufficient to direct the protein to lysosomes where it is degraded. Future work may reveal that the GPP130 response evolved for the purpose of Mn homeostasis and that the mechanism of down-regulation makes use of a pre-existing quality control pathway.

2.5 MATERIALS AND METHDOS

Antibodies and other reagents. Polyclonal antibodies against GPP130 and giantin (Mukhopadhyay *et al.*, 2010) and monoclonal antibodies against GPP130 and GFP are described (Puri *et al.*, 2002; Mukhopadhyay *et al.*, 2010). Horseradish peroxidase-conjugated goat anti-rabbit or anti-mouse secondary antibodies were used at 1:3000 for immunoblots (Bio-Rad, Hercules, CA). Alexa Fluor 488- and Alexa Fluor 568- (Invitrogen, Carlsbad, CA) were used as secondary antibodies at 1:400 for immunofluorescence. Dithiobis [succinimidyl propionate] (DSP) was from Thermo Scientific. AP (now called D/D solubilizer) was purchased from Clontech. Unless noted, other chemicals were from Fisher (Fisher Scientific, Hanover Park, IL).

Cell Culture and Transfections. HeLa cells were grown in minimum essential medium (MEM) with 100 IU/ml penicillin-G and 100 μg/ml streptomycin supplemented with 10% fetal bovine serum (Atlanta Biologicals, Lawrenceville, GA) and maintained at 37^0C in a 5% CO_2 incubator. For 20°C incubations, the cells were floated on a 20°C water bath in a cold room. For Mn treatment, culture medium was adjusted to the desired concentration using a freshly prepared 1 M stock of $MnCl_2$ in sterile water. DNA transfections were performed using the JetPEI transfection reagent (PolyPlus, Illkirch, France) according to the manufacturer's protocol. Cultures were transfected 24 h after plating and, unless noted otherwise, used for experiments 24 h after transfection.

Constructs. Chimeric constructs GP73-GPP130$_{36-175}$-GFP and GP73-GPP130$_{36-87}$-GFP are described (Mukhopadhyay et al., 2010). GP73-GPP130$_{36-107}$-GFP, GP73-GPP130$_{36-100}$-GFP, GP73-GPP130$_{36-95}$-GFP, GP73-GPP130$_{50-100}$-GFP and GP73-GPP130$_{60-100}$-GFP were created from the parent construct GP73-GPP130$_{36-175}$-GFP using a PCR-based loop-out modification of the QuikChange protocol (Stratagene, La Jolla, CA)**.** Briefly, a 5′ forward primer was designed to anneal with 18-21 base pairs on both sides flanking the region to be deleted thus creating the loop-out. A 3′ reverse primer (18-21 base pairs) was designed to anneal with a strand complementary to 3' end of the forward primer. Forward and reverse primers were designed to contain either a guanine or cytosine at each end to increase annealing. Alanine substitutions in GP73-GPP130$_{36-95}$-GFP and GP73-GPP130$_{36-175}$-GFP were introduced using the loop-out modification. All constructs maintained the integrity of the predicted coiled-coil structure based on analysis using the COILS program. Previous work describes the generation of GST-GPP130$_{36-247}$, GST-GPP130$_{36-175,}$ GST-GPP130$_{36-87}$ (Mukhopadhyay et al., 2012) and GST-GP73$_{36-195}$ (Bachert et al., 2007). GST-GPP130$_{36-175}$ (containing the $_{88}$AAAA$_{91}$ substitution) was generated using the loop-out modification. GPP130$_{1-247}$-FM-GFP was generated by subcloning the FM domain (from Man1-FM-HA, a generous gift from Dr. Alberto Luini, Instituto di Biochimica delle Proteine, Consiglio Nazionale delle Richerche, Italy (Rizzo *et al.*, 2013)) in frame after the codon for residue 247 of GPP130 and before the GFP sequence using restriction sites. All constructs were confirmed by restriction analysis and sequencing.

Trafficking assay. Approximately 24 h post-transfection, the media was adjusted to 100 μg/mL cycloheximide for 2 h and then adjusted to 500 μM $MnCl_2$ for another 2 h. The cells were then fixed and analyzed by immunofluorescence to detect GFP and endogenous GPP130 as described below.

Protein purification and Mn binding assays. GST and GST fusion proteins were expressed and purified from bacteria as described (Guo *et al.*, 2008). The purified proteins were dialyzed into PBS at pH 7.4 containing 0.1% β-mercaptoethanol or Good's buffer (10 mM HEPES, 115 mM NaCl, 2.4 mM K_2HPO_4, pH 7.4) with 0.1% β-mercaptoethanol. Stripped NTA-agarose beads were generated by washing Ni-NTA agarose beads (Invitrogen) with 5 volumes of water, 3 volumes of 2% SDS followed by a dehydration/rehydration series of 1 volume each of 25%, 50% and 75% EtOH, 5 volumes of 100% EtOH, 1 volume of 75%, 50% and 25% EtOH, 5 volumes of water and then 5 volumes of 100 mM EDTA, pH8.0. Color change (blue to white) accompanied removal of Ni. The stripped NTA agarose beads were then rotated with 50 mM $MnCl_2$ for 1 hour at 4°C, followed by centrifugation and resuspension in water in preparation for use the same day. For binding, either 10 μL of Mn beads were washed and incubated with 10 μg of the indicated protein in PBS or 5 μL of Mn beads were washed and incubated with 0.5 μg of the indicated protein in Good's buffer. The reaction (50 μL total volume) was rotated for 30 min at 4°C. Beads were collected and twice washed with binding buffer containing 0.1% Triton X100 using pulse spins and aspiration of the supernatants with a 25-gauge needle. A final wash with binding buffer only was followed by boiling in reducing sample buffer, SDS-PAGE,

Coomassie staining, image capture (Fujifilm Luminescent Image Analyzer, LAS-3000) and quantification using ImageJ. To determine the concentration dependence of binding, 5 µl aliquots of stripped NTA-agarose beads were rotated with various concentrations of $MnCl_2$ for 1 h at 4°C and then supplemented with 0.5 µg of GST-GPP130$_{36-247}$ and rotated for an additional 30 min at 4°C. Binding was carried out in Good's buffer with a 30 µL reaction volume achieving the indicated final $MnCl_2$ concentration. Washing and analysis were as before except that nonlinear regression analysis was performed using Prism (GraphPad Software Inc., La Jolla, CA).

Light scattering assay. Purified proteins (5 µM, 10 µl final volume) were incubated with various concentrations of $MnCl_2$ for 5 min at room temperature in either PBS or Good's buffer. Absorbance was then determined at 360 nm using ND-1000 UV-Vis spectrophotometer (NanoDrop,Wilmington, DE). For the reversibility test, after the initial 5 min, an equal concentration of EDTA was added for an additional 5 min.

Velocity gradient sedimentation assays. Purified proteins (10 µg) were layered on top of sucrose gradients prepared in PBS with or without 1 mM $MnCl_2$ and consisting of a 1 mL 40% cushion overlaid with 1 mL steps of 22.5% and 10%. Centrifugation was at 55,000 rpm in a SW50.1 rotor (Beckman Coulter) rotor for 12 h at 4°C. Fractions (500 µL) were collected from the top with a pipette and analyzed by Coomassie and quantified as described (Mukhopadhyay et al., 2013). For cell extract analysis, transfected or control cells were treated with 0 or

500 μM Mn for 3 h at 37°C. For each gradient, cells in two 10 cm dishes were then washed with PBS, trypsinized, collected by centrifugation for 2 min at 450 x *g* resuspended in 500 μL PBS which was then adjusted to 0.5 mM DSP and rotated at 37°C for 45 min. The reaction was quenched by adjustment to 50 mM Tris on ice for 15 min. For cells exposed to Mn at 20°C, the extracts were prepared in the same way except that they were removed from plates by scraping while on ice and the crosslinking was carried out at 20°C. After quenching, the cells were collected and lysed in RIPA buffer (25mM pH7.4, 150mM NaCl, 1% NP-40, 0.5% sodium deoxycholate, 0.1% SDS and 0.1% β-mercaptoethanol, 10μg/mL leupeptin, 10μg/mL pepstatin and 1mM PMSF) using 50 passes through a 25-gauge needle. The extract was clarified in a microfuge at 15,000 rpm for 15 min at 4°C and layered on 10%-40% linear sucrose gradient in RIPA buffer. Centrifugation was at 50,000 rpm in the SW50.1 rotor for 1.5 h at 4°C. Fractions (500 μL) were collected from the bottom using tubing and a peristaltic pump. Remaining material at the bottom was resuspended in RIPA buffer. Immunoblot analysis was carried out on 20% of each fraction and the entire pellet using enhanced chemiluminescence, image capture (Fujifilm Luminescent Image Analyzer, LAS-3000) and quantification (ImageGauge software, Fujifilm).

Controlled polymerization. Cells were transfected with GPP130$_{1-247}$-FM-GFP and after 16-18 h they were placed in fresh media containing 1μM AP for 24 h followed by another change to media containing 1 μM AP and 100 μg/mL cycloheximide for 30 minutes. Next the cells were incubated in media containing

only 100 μg/mL cycloheximide for various times prior to fixation and imaging. Only cells exhibiting moderate expression levels were analyzed.

Microscopy. Immunofluorescence was performed on cells fixed with 3% PFA as described (Mukhopdhyay et al., 2010) using Alexa Fluor 488 and 568 secondary antibodies (Invitrogen). Images were captured using a spinning-disk confocal scan head microscope equipped with a three-line laser (Qioptiq), independent excitation and emission filter wheels (PerkinElmer Life and Analytical Sciences, Boston, MA) and a 12-bit Orca ER digital camera (Hamamatsu Photonics, Bridgewater, NJ) mounted on an Axiovert 200 microscope with a 100X, 1.4 numerical aperture oil immersion objective (Carl Zeiss, Thornwood, NY). Sections encompassing the cells were acquired at 0.3 μm steps using MicroManager software (http://www.micro-manager.org/). To highlight cytoplasmic puncta, images presented in the figures are maximum value projections that have been uniformly thresholded after background subtraction. FRAP experiments were carried out with the Andor iQ2 spinning-disk confocal system. Stacks of Z-slices were acquired at 10 s intervals for 1 min prior to photobleaching to establish a baseline. GFP was bleached using 27.3 mW of 488-nm laser power for 20 μs/pixel repeated 60 times. Fluorescence recovery was followed at 10 s intervals for 10 min following photobleaching.

Image Analysis. Immunofluorescence images were analyzed using ImageJ (National Institutes of Health, Bethesda, MD, http://imagej.nih.gov/ij/) as described (Mukhopadhyay *et al.*, 2010). To measure fluorescence per cell,

background was subtracted from each Z section and average value projections were created. Cells were outlined using the Gaussian blur filter and mean fluorescence was measured using the Measure plugin of ImageJ. The number of cytoplasmic punctae per cell was determined using the Analyze Particle plugin of ImageJ (particle range setting of 10-100 pixels) from maximum value projections that were uniformly thresholded after background subtraction. FRAP analysis in ImageJ was performed on average Z-projections of background subtracted slices. The total fluorescence value within the bleached region was normalized to the total cellular fluorescence at each time point to correct for photobleaching due to imaging using the following equation:

$$FRAP\ \ normalization\ =\ \left(\frac{Roi_{(n)}\ /\ Roi_{(-1)}}{Total_{(n)}\ /\ Total_{(-1)}}-\frac{Roi_{(0)}\ /\ Roi_{(-1)}}{Total_{(0)}\ /\ Total_{(-1)}}\right)\ \div\ \left(1-\frac{Roi_{(0)}\ /\ Roi_{(-1)}}{Total_{(0)}\ /\ Total_{(-1)}}\right)$$

Statistical Analysis. Comparisons between any two groups were performed using two-tailed Student's t test assuming equal variances. P values of <0.05 were considered statistically significant unless otherwise noted.

2.6 REFERENCES

Anderson, E.D., VanSlyke, J.K., Thulin, C.D., Jean, F., and Thomas, G. (1997). Activation of the furin endoprotease is a multiple-step process: requirements for acidification and internal propeptide cleavage. EMBO J *16*, 1508-1518.

Beddoe, T., Paton, A.W., Le Nours, J., Rossjohn, J., and Paton, J.C. (2010). Structure, biological functions and applications of the AB5 toxins. Trends Biochem Sci *35*, 411-418.

Berwick, M.R., Lewis, D.J., Jones, A.W., Parslow, R.A., Dafforn, T.R., Cooper, H.J., Wilkie, J., Pikramenou, Z., Britton, M.M., and Peacock, A.F. (2014). De novo design of Ln(III) coiled coils for imaging applications. J Am Chem Soc *136*, 1166-1169.

Borgstahl, G.E., Parge, H.E., Hickey, M.J., Beyer, W.F., Jr., Hallewell, R.A., and Tainer, J.A. (1992). The structure of human mitochondrial manganese superoxide dismutase reveals a novel tetrameric interface of two 4-helix bundles. Cell *71*, 107-118.

Chakraborty, S., Touw, D.S., Peacock, A.F., Stuckey, J., and Pecoraro, V.L. (2010). Structural comparisons of apo- and metalated three-stranded coiled coils clarify metal binding determinants in thiolate containing designed peptides. J Am Chem Soc *132*, 13240-13250.

Colomer, V., Kicska, G.A., and Rindler, M.J. (1996). Secretory granule content proteins and the luminal domains of granule membrane proteins aggregate in vitro at mildly acidic pH. J Biol Chem *271*, 48-55.

Culotta, V.C., Yang, M., and Hall, M.D. (2005). Manganese transport and trafficking: lessons learned from Saccharomyces cerevisiae. Eukaryot Cell *4*, 1159-1165.

Emr, S., Glick, B.S., Linstedt, A.D., Lippincott-Schwartz, J., Luini, A., Malhotra, V., Marsh, B.J., Nakano, A., Pfeffer, S.R., Rabouille, C., Rothman, J.E., Warren, G., and Wieland, F.T. (2009). Journeys through the Golgi--taking stock in a new era. J Cell Biol *187*, 449-453.

Endo, Y., Tsurugi, K., Yutsudo, T., Takeda, Y., Ogasawara, T., and Igarashi, K. (1988). Site of action of a Vero toxin (VT2) from Escherichia coli O157:H7 and of Shiga toxin on eukaryotic ribosomes. RNA N-glycosidase activity of the toxins. Eur J Biochem *171*, 45-50.

Fraser, M.E., Chernaia, M.M., Kozlov, Y.V., and James, M.N. (1994). Crystal structure of the holotoxin from Shigella dysenteriae at 2.5 A resolution. Nat Struct Biol *1*, 59-64.

Freedman, S.D., and Scheele, G.A. (1993). Regulated secretory proteins in the exocrine pancreas aggregate under conditions that mimic the trans-Golgi network. Biochem Biophys Res Commun *197*, 992-999.

Guo, Y., Punj, V., Sengupta, D., and Linstedt, A.D. (2008). Coat-tether interaction in Golgi organization. Mol Biol Cell *19*, 2830-2843.

Jensen, L.T., Carroll, M.C., Hall, M.D., Harvey, C.J., Beese, S.E., and Culotta, V.C. (2009). Down-regulation of a manganese transporter in the face of metal toxicity. Mol Biol Cell *20*, 2810-2819.

Johannes, L., and Wunder, C. (2011). Retrograde transport: two (or more) roads diverged in an endosomal tree? Traffic *12*, 956-962.

La Fontaine, S., and Mercer, J.F. (2007). Trafficking of the copper-ATPases, ATP7A and ATP7B: role in copper homeostasis. Arch Biochem Biophys *463*, 149-167.

Mallard, F., and Johannes, L. (2003). Shiga toxin B-subunit as a tool to study retrograde transport. Methods Mol Med *73*, 209-220.

Mukhopadhyay, S., Bachert, C., Smith, D.R., and Linstedt, A.D. (2010). Manganese-induced trafficking and turnover of the cis-Golgi glycoprotein GPP130. Mol Biol Cell *21*, 1282-1292.

Mukhopadhyay, S., and Linstedt, A.D. (2011). Identification of a gain-of-function mutation in a Golgi P-type ATPase that enhances Mn2+ efflux and protects against toxicity. Proc Natl Acad Sci U S A *108*, 858-863.

Mukhopadhyay, S., and Linstedt, A.D. (2012). Manganese blocks intracellular trafficking of Shiga toxin and protects against Shiga toxicosis. Science *335*, 332-335.

Mukhopadhyay, S., and Linstedt, A.D. (2013). Retrograde trafficking of AB(5) toxins: mechanisms to therapeutics. J Mol Med (Berl) *91*, 1131-1141.

Mukhopadhyay, S., Redler, B., and Linstedt, A.D. (2013). Shiga toxin-binding site for host cell receptor GPP130 reveals unexpected divergence in toxin-trafficking mechanisms. Mol Biol Cell *24*, 2311-2318.

Polishchuk, R., and Lutsenko, S. (2013). Golgi in copper homeostasis: a view from the membrane trafficking field. Histochem Cell Biol *140*, 285-295.

Puri, S., Bachert, C., Fimmel, C.J., and Linstedt, A.D. (2002). Cycling of early Golgi proteins via the cell surface and endosomes upon lumenal pH disruption. Traffic *3*, 641-653.

Reddi, A.R., Jensen, L.T., and Culotta, V.C. (2009). Manganese homeostasis in Saccharomyces cerevisiae. Chem Rev *109*, 4722-4732.

Rizzo, R., Parashuraman, S., Mirabelli, P., Puri, C., Lucocq, J., and Luini, A. (2013). The dynamics of engineered resident proteins in the mammalian Golgi complex relies on cisternal maturation. J Cell Biol *201*, 1027-1036.

Sandvig, K., Bergan, J., Dyve, A.B., Skotland, T., and Torgersen, M.L. (2010). Endocytosis and retrograde transport of Shiga toxin. Toxicon *56*, 1181-1185.

Shennan, K.I., Taylor, N.A., and Docherty, K. (1994). Calcium- and pH-dependent aggregation and membrane association of the precursor of the prohormone convertase PC2. J Biol Chem *269*, 18646-18650.

Sullivan, J.A., Lewis, M.J., Nikko, E., and Pelham, H.R. (2007). Multiple interactions drive adaptor-mediated recruitment of the ubiquitin ligase rsp5 to membrane proteins in vivo and in vitro. Mol Biol Cell *18*, 2429-2440.

Youker, R.T., Bruns, J.R., Costa, S.A., Rbaibi, Y., Lanni, F., Kashlan, O.B., Teng, H., and Weisz, O.A. (2013). Multiple motifs regulate apical sorting of p75 via a mechanism that involves dimerization and higher-order oligomerization. Mol Biol Cell *24*, 1996-2007.

CHAPTER 3

Induced-Oligomerization Targets Golgi Proteins for Degradation in Lysosomes

3.1 ABSTRACT

Manganese (Mn) protects cells against forms of Shiga toxin by down-regulating the cycling Golgi protein GPP130. Down-regulation occurs when Mn binding causes GPP130 to oligomerize and traffic to lysosomes. To determine how GPP130 is redirected to lysosomes, we tested the role of GGA1 and clathrin, which mediate sorting in the canonical Golgi-to-lysosome pathway. GPP130 oligomerization was induced using either Mn or a self-interacting version of the FKBP domain. Inhibition of GGA1 or clathrin specifically blocked GPP130 redistribution suggesting recognition of the aggregated GPP130 by the GGA1/clathrin sorting complex. Unexpectedly, however, GPP130's cytoplasmic domain was not required and redistribution also occurred after removal of GPP130 sequences needed for its normal cycling. Therefore, to test whether aggregate recognition might be a general phenomenon rather than one involving a specific GPP130 determinant, we induced homo-oligomerization of two unrelated Golgi-targeted constructs using the FKBP strategy. These were targeted to the *cis* and *trans* Golgi respectively using domains from mannosidase-1 and galactosyltransferase. Significantly, upon oligomerization, each redistributed to peripheral punctae and was degraded. This occurred in the absence of detectable UPR activation. These findings suggest the unexpected presence of quality control in the Golgi that recognizes aggregated Golgi proteins and targets them for degradation in lysosomes.

3.2 INTRODUCTION

The Golgi membrane protein GPP130 normally cycles between its steady state location in the *cis* Golgi and endosomes (Puri *et al.*, 2002). An increase in Golgi Mn causes it to leave this itinerary and instead traffic to lysosomes where it is degraded (Mukhopadhyay *et al.*, 2010). Although the role of GPP130 is unknown, this trafficking switch is fortuitous because the bacterially produced Shiga toxin and Shiga toxin 1 (STx/STx1), which cause severe diarrhea and fatal kidney failure (Beddoe *et al.*, 2010) depend on GPP130 for their invasion of host cells (Natarajan and Linstedt, 2004; Mukhopadhyay and Linstedt, 2012). The toxins bind GPP130 in endosomes and piggyback a ride to the Golgi, which allows them to escape degradation in the lysosome (Mukhopadhyay and Linstedt, 2012; Mukhopadhyay *et al.*, 2013). Indeed, Mn-induced down-regulation of GPP130 prevents STx/STx1 trafficking and Mn protects cells and mice against Shiga toxicosis (Mukhopadhyay and Linstedt, 2012).

The switch in sorting fate of GPP130 caused by Mn is an instance of an important general regulatory mechanism in which sorting during membrane trafficking is used as a control point. The best-known examples of this type of sorting switch are those induced by ligand binding to cell surface receptors. Ligand binding induces conformational changes and/or post-translational modifications of cytoplasmically disposed sorting signals. This alters the interaction of these signals with vesicle coat adaptors driving endocytosis (Traub and Bonifacino, 2013; Piper *et al.*, 2014). A related scenario takes place when cholesterol regulates the ER exit of the SCAP/SREBP complex. Cholesterol binding changes SCAP's conformation leading to binding of another factor that masks SCAP's sorting signal for ER exit (Brown and Goldstein,

1997; Sun *et al.*, 2007). There are also disease-related examples. Human immunodeficiency virus type 1 protein Nef alters the sorting of the major histocompatibility complex-1 by mediating the indirect interaction of MHC1 with the AP-1 adaptor protein at the trans Golgi network (TGN) (Le Gall *et al.*, 1998). Mutation of the amyloid precursor protein in Alzheimer's disease blocks its interaction with the adaptor AP-4 at the TGN resulting in greater cleavage to the pathogenic amyloid-β peptide (Roeth *et al.*, 2004). Control of sorting is also a critical aspect of metal ion homeostasis and this may be the proper context in which to place Mn control of GPP130 trafficking. Similar to Mn-induced GPP130 trafficking, elevated copper causes redistribution of the Golgi proteins ATP7A and ATP7B, which are copper translocating pumps. The pumps move from the TGN to the cell surface where they expel excess copper (Polishchuk and Lutsenko, 2013).

For each particular case of regulated sorting, understanding the underlying mechanism responsible for enrichment of the sorted membrane protein is critical to elucidating the switch. As in several of the above examples, local enrichment is typically achieved by direct or adaptor-mediated interactions of the sorted cargo with an assembling vesicle coat complex resulting in selective export in a budding vesicle or membrane tubule (Bonifacino and Glick, 2004; Traub and Bonifacino, 2013). Alternatively, local enrichment may be driven by accumulation in particular lipid domains (Surma *et al.*, 2012) or interaction with localized domains of assembled cytoskeleton (Irannejad and von Zastrow, 2014).

Significantly, recent work indicates that the switch in GPP130 sorting may involve a novel mechanism for its local enrichment in the plane of the membrane.

When Mn is elevated, the GPP130 lumenal stem domain binds Mn and this binding causes GPP130 oligomerization/aggregation that is required and sufficient for its altered sorting (Tewari *et al.,* 2014). Here we sought to extend our understanding of this pathway by answering the following questions. Is a TGN-localized vesicle coat complex adaptor involved? If so, are specific sequence elements in GPP130 required or is this sorting switch something more general such that it acts on any oligomerized/aggregated Golgi protein? Our work implicates γ-adaptin homologous ARF-interacting protein 1 (GGA1) and clathrin in a sorting switch that appears general to Golgi proteins.

3.3 RESULTS

Role of the canonical Golgi-lysosome pathway in oligomerization-induced trafficking

Mn-induced GPP130 trafficking involves redistribution to multivesicular bodies (MVBs) where GPP130 is internalized to intraluminal vesicles and then appearance in LAMP2 positive lysosomes where its degradation is blocked by leupeptin inhibition of lysosomal hydrolases (Mukhopadhyay *et al.*, 2010). The redistribution is insensitive to a dominant negative (DN) version of dynamin, microtubule disruption or DN-Rab5 indicating that neither endocytosis nor early endosome trafficking are involved (Mukhopadhyay *et al.*, 2010). In contrast, it is blocked by DN-Rab7-T22N (Mukhopadhyay *et al.*, 2010), which inhibits trafficking from MVBs to lysosomes (Bucci *et al.*, 2000; Vanlandingham and Ceresa, 2009). The canonical route from the Golgi towards lysosomes is mediated by Golgi associated, GGA1 and clathrin (Black and Pelham, 2000; Puertollano *et al.*, 2001b; Zhu *et al.*, 2001). Thus, we employed a DN version of GGA1 and a small molecule inhibitor of clathrin to test whether the oligomerization-induced trafficking of GPP130 occurs via this canonical route.

For GGA1, HeLa cells were transfected with either a wildtype version or a version lacking the clathrin binding domains (GGA1-DN), which is known to block export of lysosome-directed cargo from the TGN (Puertollano *et al.*, 2001b). The constructs were GFP tagged and each was Golgi-localized upon expression (Fig 3-1A, row 1-2). Cells were then treated with Mn for 5 h and GPP130 redistribution was determined. In cells expressing the wildtype GGA1, GPP130 moved from it's

predominant Golgi localization to peripheral punctae (Fig 3-1A, row 3) indicating movement to lysosomes as previously described (Mukhopadhyay *et al.*, 2010). In contrast, cells expressing GGA1-DN showed little or no GPP130 redistribution (Fig 3-1A, row 4). (Note that thresholding of the GPP130 channel (last column) is presented to illustrate the peripheral punctae, which are dim due to GPP130 degradation. For thresholding and all other analysis within an experiment, identical parameters were used to allow direct comparison.)

Monensin treatment provided a convenient control to test the specificity of the GGA1 inhibition. Monensin is a proton ionophore that neutralizes acidic compartments (Tartakoff, 1983) causing GPP130 redistribution to endosomes presumably because GPP130 endosome-to-Golgi retrieval is pH-dependent (Linstedt *et al.,* 1997; Starr *et al.,* 2007). Thus, TGN export of GPP130 upon monensin-treatment is expected to occur via a distinct pathway from lysosome-directed cargo and occur independently of GGA1. Indeed, the marked appearance of GPP130 in peripheral endosomes after monensin addition was unabated by expression of either wildtype or GGA1-DN (Fig 3-1B).

The specific dependence of Mn-induced GPP130 redistribution on GGA1 was confirmed by image analysis for independent experiments quantifying the number of distinct GPP130 punctae per cell. A significant block was evident for GGA1-DN after Mn treatment but not after monensin treatment (Fig 3-1C). Further, the loss of total GPP130 fluorescence per cell after Mn treatment, which is a measure of its degradation in lysosomes (Mukhopadhyay *et al.*, 2010), was abrogated in cells expressing GGA1-DN (Fig 3-1D).

Figure 1

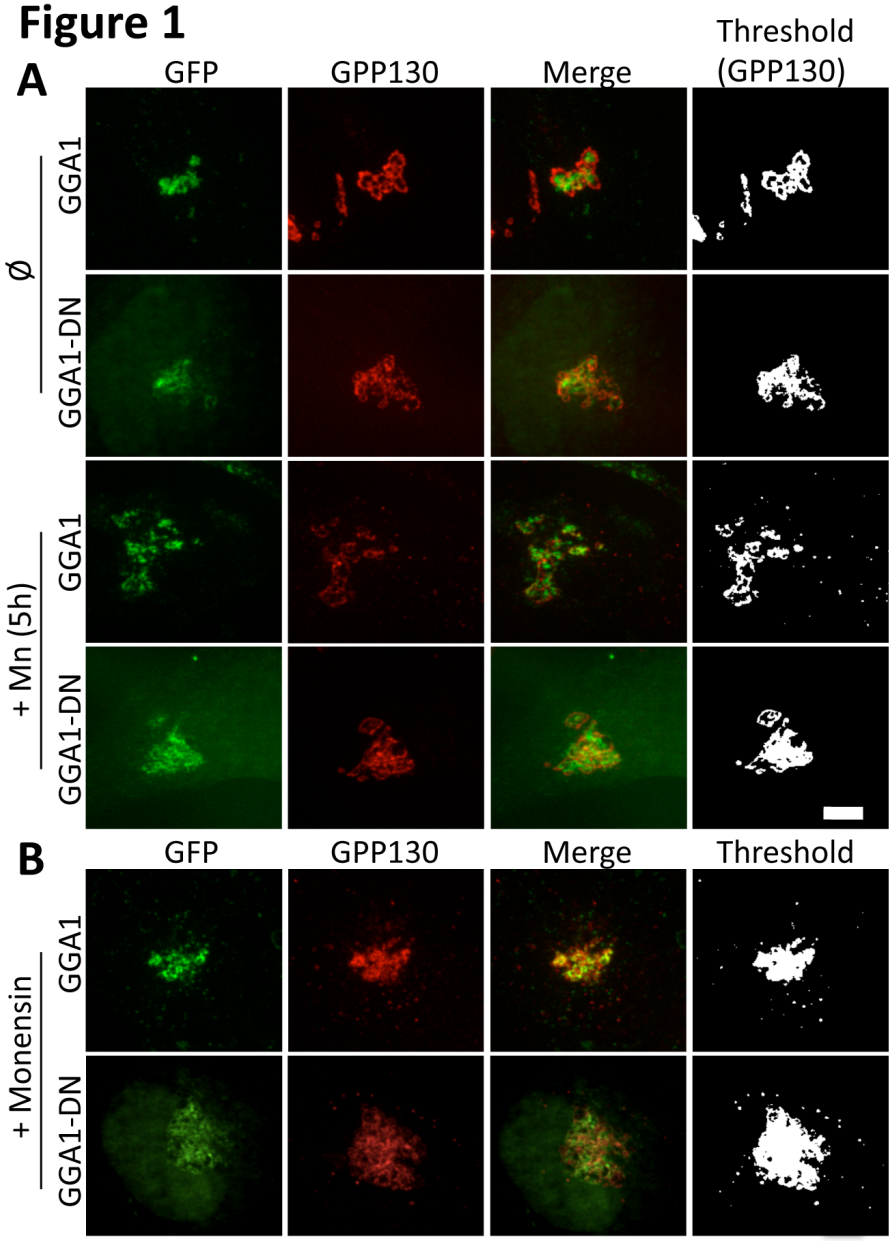
A
GFP
GPP130
Merge
Threshold (GPP130)
Ø
GGA1
GGA1-DN
+ Mn (5h)
GGA1
GGA1-DN
B
GFP
GPP130
Merge
Threshold
+ Monensin
GGA1
GGA1-DN

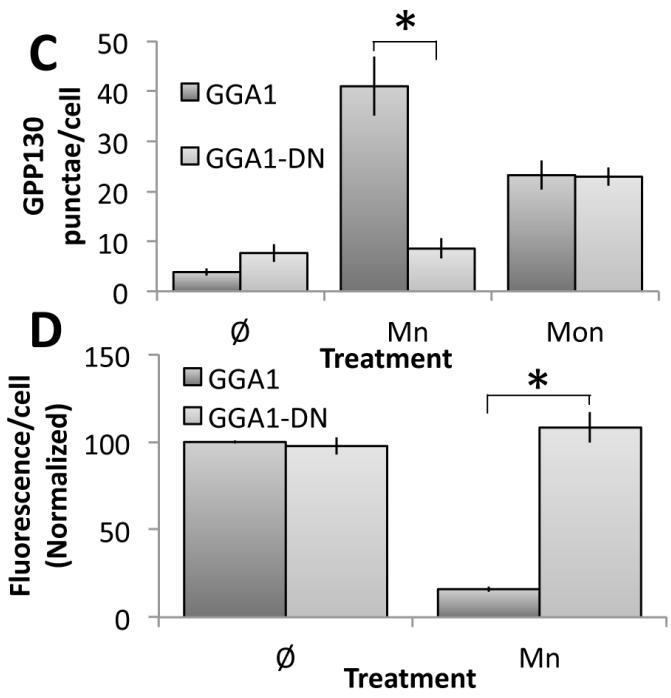

Figure 3-1. Dominant negative GGA1 blocks Mn-induced GPP130 trafficking.

(A) Cells were transfected with GFP-tagged GGA1 or GGA1-DN and then either left untreated (Ø) or treated with Mn for 5 h. Images show GFP fluorescence from the transfected proteins and anti-GPP130 staining with the final panel using uniform thresholding of the GPP130 image to aid visualization of small punctae. Note that GGA1-DN blocked GPP130 appearance in punctae. Bar=5μm. (B) Cells expressing GGA1 or GGA1-DN were treated with monensin for 30 min to induce GPP130 trafficking to endosomes. (C). Quantified appearance of GPP130 in peripheral punctae of cells expressing GGA1 or GGA1-DN after Mn or monensin (Mon) treatment (mean±SEM, n=3, >10 cells per experiment, *$p<0.05$). (D) Total cell fluorescence of GPP130 in cells expressing GGA1 or GGA1-DN before or after Mn (mean±SEM, n=3, >10 cells per experiment).

Given these results for Mn-induced GPP130 redistribution, we also tested the role of GGA1 for GPP130-FM. GPP130-FM is a previously characterized construct (Tewari *et al.,* 2014) in which GPP130 residues 1-247 are followed by 3 copies of a modified version of the FKBP12 domain termed FM (after its F36M substitution). The FM domain self-interacts in a manner that is inhibited by the drug AP21998 (AP), an analogue of rapamycin. Washout of AP forms large complexes due to multiplexing of the three FM domains and, upon AP washout, GPP130-FM leaves the Golgi to peripheral endosomes and lysosomes where it is degraded (Tewari *et al.,* 2014). As expected, neither GGA1 nor GGA1-DN altered GPP130-FM localization before AP washout (Fig 3-2, row 1-2) and redistribution of GPP130-FM was readily apparent in cells expressing wildtype GGA1 (Fig 3-2, row 3). Interestingly, GGA1 partially redistributed along with GPP130-FM consistent with the possible persistence of a GGA1-based sorting complex associated with GPP130-FM beyond the TGN. In contrast, in cells expressing GGA1-DN the appearance of GPP130-FM in peripheral punctae was significantly reduced (Fig 3-2, row 4).

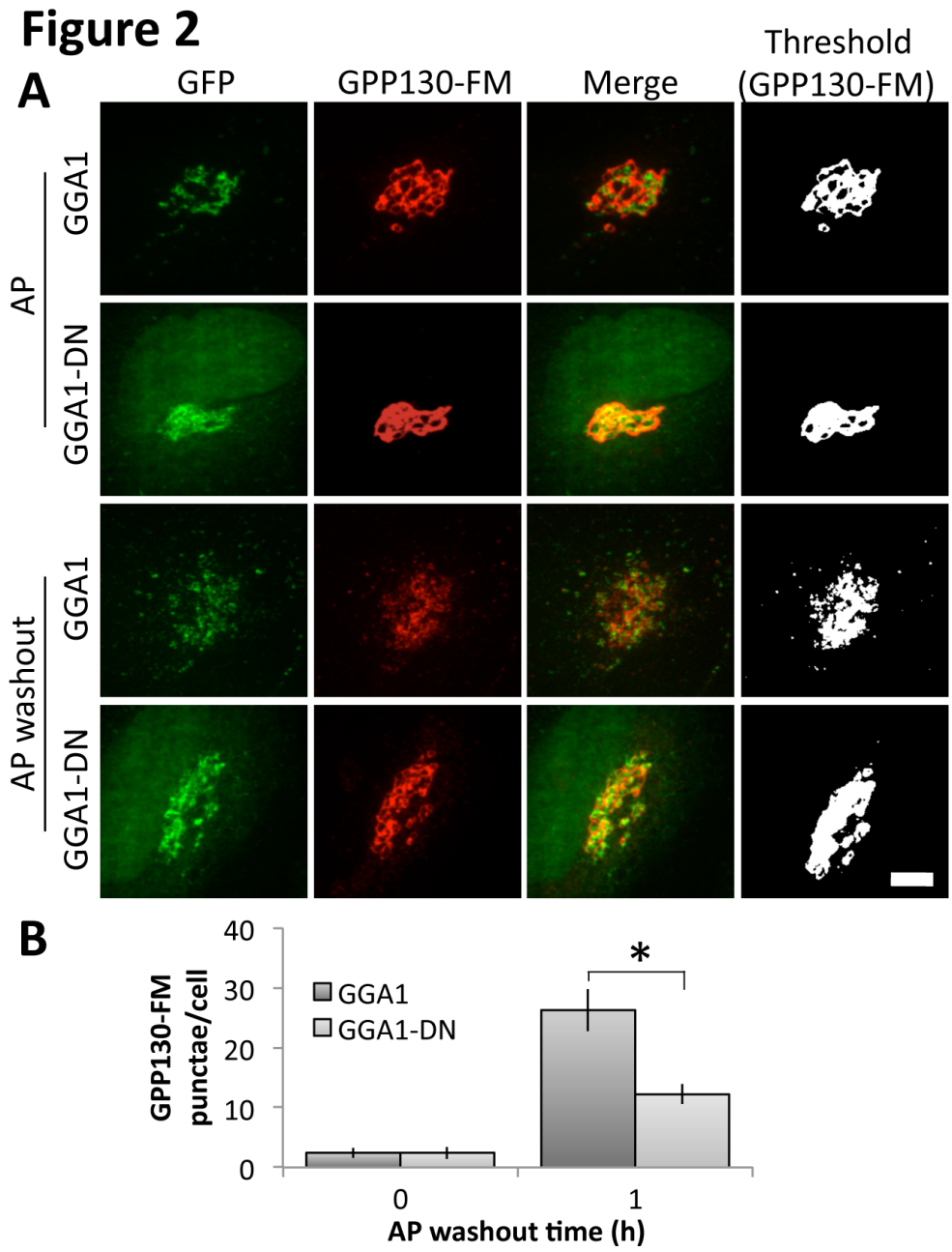

Figure 3-2. GGA1-DN blocks GPP130-FM trafficking.

(A) Cells were co-transfected with HA-tagged GPP130-FM and either GFP-tagged GGA1 or GGA1-DN and then either left in AP or treated with a 1 h AP washout. Images show GFP fluorescence from the transfected proteins and anti-HA staining with the final panel using uniform thresholding of the GPP130-FM image to aid visualization of small punctae. Bar=5μm. (B) Quantified appearance of GPP130 in peripheral punctae of cells expressing GGA1 or GGA1-DN after 0 or 1 h of AP washout (mean±SEM, n=3, >10 cells per experiment, *p<0.05).

Dependence on GGA1 implies a role for clathrin. As a test we used treatment with Pitstop®2, a selective clathrin inhibitor. Pitstop®2 occupies the clathrin terminal domain groove preventing this domain's interaction with clathrin box ligands, which stalls clathrin coated pit dynamics (von Kleist et al., 2011). Only short-term treatments were used to minimize indirect and toxic effects of the drug. HeLa cells expressing GPP130-FM were transferred to serum free medium (serum interferes with Pitstop®2) in the continued presence of AP. Then, the washout of AP was carried out for 10 min with media containing either DMSO alone or DMSO containing Pitstop®2. Whereas a clear appearance in peripheral punctae was noted in control cells, no such redistribution occurred in cells treated with the clathrin inhibitor and this was confirmed by image analysis (Fig 3-3). Taken together, the data in this section indicate that trafficking of oligomerized GPP130 to lysosomes requires TGN export that is GGA1 and clathrin dependent.

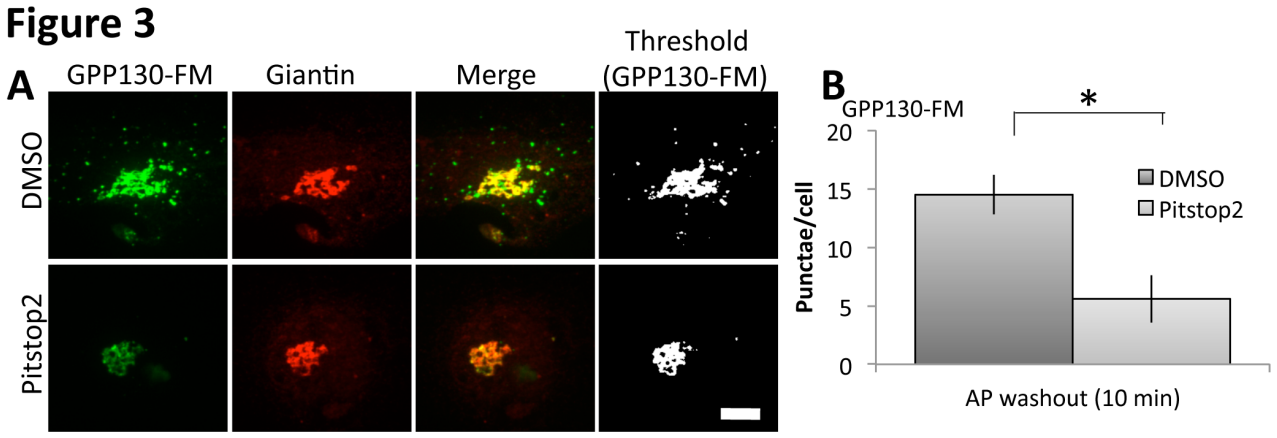

Figure 3-3. Clathrin inhibitor blocks oligomer-induced GPP130 trafficking.

(A) GPP130-FM transfected cells in the presence of AP were washed into serum-free media lacking AP and containing either vehicle alone (DMSO) or vehicle containing the clathrin inhibitor Pitstop2.

The cells were fixed and analyzed after 10 min to minimize indirect and toxic effects of Pitstop2. Images show GFP fluorescence from GPP130-FM and anti-giantin staining to mark the Golgi as well as thresholded GPP130 images to mark cytoplasmic punctae. Note that Pitstop2 blocked GPP13-FM appearance in punctae. Bar=5μm. (B) Quantified appearance of GPP130-FM in peripheral punctae of control and Pitstop2-treated cells after AP washout (mean±SEM, n=3, >10 cells per experiment, *p<0.05).

Sorting signals for oligomerization-induced GPP130 trafficking?

GGA1 functions as a coat complex adaptor by interacting with cytoplasmic motifs in diverse cargo (Puertollano *et al.,* 2001b; He *et al.,* 2002). Although GPP130 has a complex trafficking itinerary that involves multiple distinct domains, its cytoplasmic domain has not yet been implicated in it's targeting. Because it is not needed for Golgi targeting, we could test the role of the cytoplasmic domain in oligomerization-induced trafficking of GPP130. We deleted residues 2-11 of the 12 residue cytoplasmic domain in our FM-domain GPP130 construct to create ∆cyto-GPP130-FM. As expected, the construct was localized to the Golgi in the continued presence of AP, whereas after AP washout, ∆cyto-GPP130-FM redistributed to peripheral punctae in a manner indistinguishable from wildtype (Fig 3-4A). Image analysis confirmed the significant increase in punctae (Fig 3-4B) as well as the loss of total staining over time reflecting degradation (Fig 3-4C). Thus, the cytoplasmic domain of GPP130 is not needed for its oligomerization-induced trafficking.

Figure 4

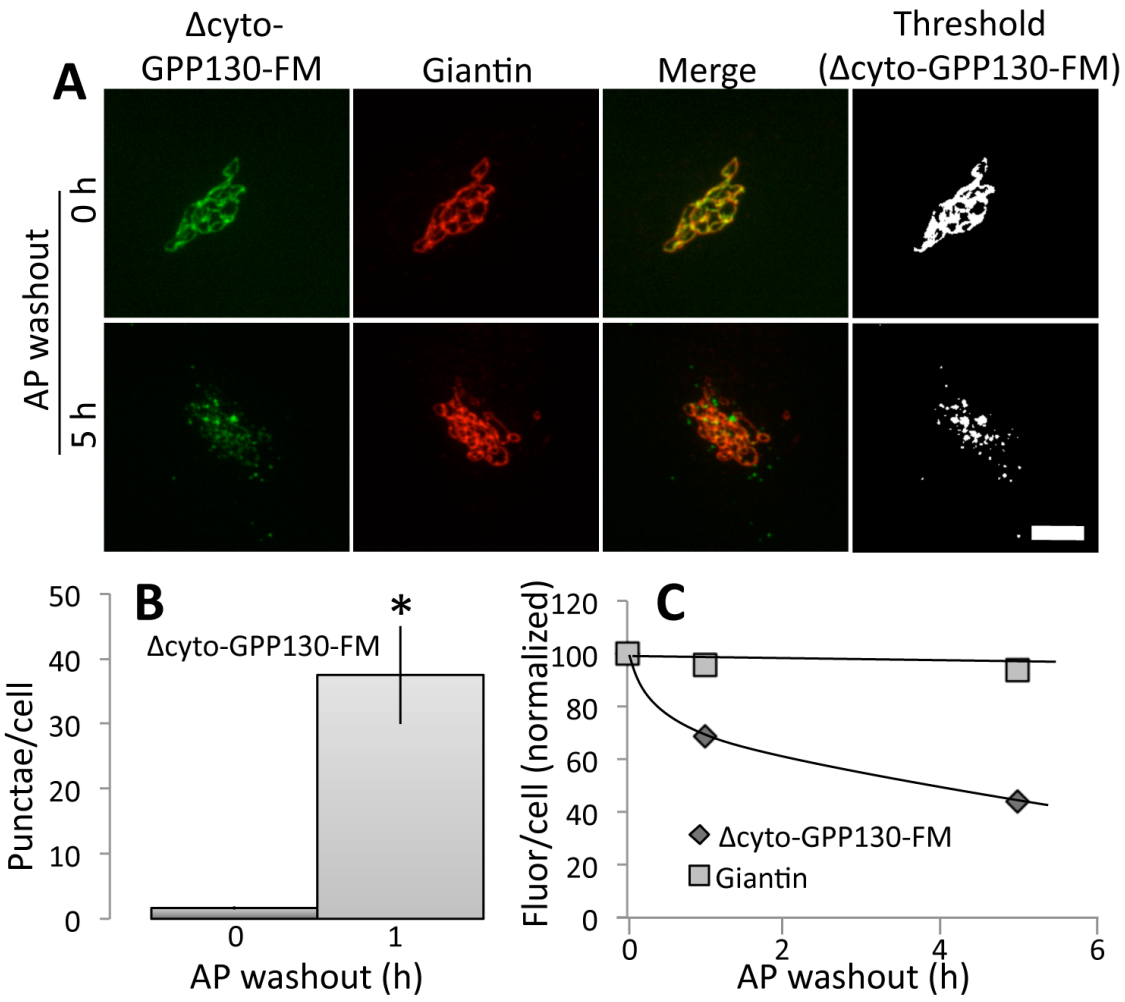

Figure 3-4. Oligomer-induced GPP130 trafficking is independent of its cytoplasmic domain.

(A) Cells were transiently transfected with Δcyto-GPP130-FM in the presence of AP and then examined at the indicated times after AP washout. Images show GFP fluorescence from Δcyto-GPP130-FM and anti-giantin staining to mark the Golgi. The final panels present the GPP130 images after uniform thresholding. Note redistribution of Δcyto-GPP13-FM. Bar=5μm. (B) Quantified appearance of Δcyto-GPP13-FM in peripheral punctae at 0 and 1 h after AP washout (mean±SEM, n=3, >10 cells per experiment, *p<0.01). (C) Determination of total fluorescence per cell after AP washout normalized to average value before AP washout (mean±SEM, n=3, >10 cells per experiment).

Next, we turned our attention to the GPP130 lumenal coiled-coil domain, which contains sequence elements that independently mediate Shiga toxin binding and Mn binding as well as Golgi targeting and endosome cycling (Bachert *et al.,* 2001; Mukhopadhyay *et al.,* 2010; Tewari *et al.,* 2014). The entire coiled-coil stretches from residues 36 to 245. Previous work indicated that a deletion of 88-245 shifts the steady state location of the protein to the *trans* Golgi, blocks it's cycling to endosomes, and blocks it's Mn responsiveness (Bachert *et al.,* 2001; Mukhopadhyay *et al.,* 2010). Therefore, we tested a GPP130-$_{1\text{-}87}$-FM construct to see if it retained the oligomerization induced trafficking response. The construct was Golgi localized before AP washout and, upon washout, it moved into peripheral punctae ultimately undergoing degradation (Fig 3-5A). Also shown are the quantified results for both its appearance in peripheral punctae (Fig 3-5B) and its loss of staining over time (Fig 3-5C). Thus, even without most of its coiled-coil stem domain, GPP130 underwent oligomerization induced trafficking and degradation. We reasoned that further deletions might be problematic due to the requirement for Golgi targeting in any construct to be tested. Also, we began to consider the possibility that the response might not be specific to GPP130 but rather part of a general pathway in the Golgi. Therefore, we next tested the behavior of *cis* and *trans* Golgi markers after their forced oligomerization.

Figure 5

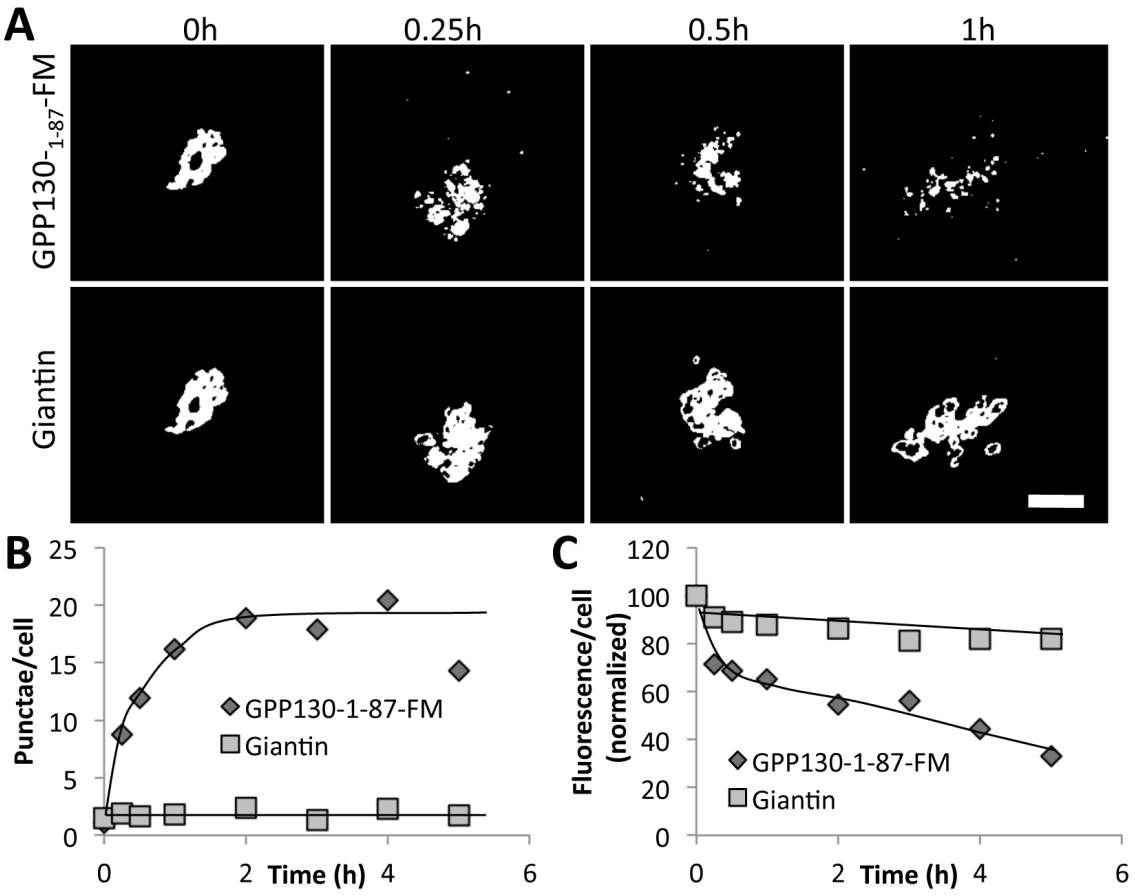

Figure 3-5. Redistribution of truncated GPP130-FM.

(A) Cells expressing GPP130-$_{1-87}$-FM (cycling deficient and Mn-insensitive) were incubated in the absence of AP for the indicated times. Images show thresholded GFP fluorescence from GPP130-$_{1-87}$-FM and anti-giantin staining to mark the Golgi. Note redistribution and then loss of GPP130-$_{1-87}$-FM. Bar=5μm. (B) Quantified appearance of GPP130-$_{1-87}$-FM in peripheral punctae after AP washout (mean±SEM, n=3, >10 cells per experiment). (C) Total GPP130-$_{1-87}$-FM or giantin fluorescence as a percent of starting value and at the indicated times of AP washout (mean±SEM, n=3, >10 cells per experiment).

Induced oligomerization causes lysosomal targeting of other Golgi proteins

We first studied the *cis* Golgi enzyme mannosidase-1 because a suitable construct (Man1-FM) had already been characterized in which tandem copies of the FM domain and an HA tag were appended to the C-terminus of a truncated mouse α-1,2 mannosidase-1B comprised of its cytoplasmic, transmembrane and stem domains (Rizzo *et al.,* 2013). The construct shows normal *cis* Golgi localization in the presence of AP and migration to the *trans* Golgi after a short AP washout (Rizzo *et al.,* 2013).

In our experiments, HeLa cells were transfected with the Man1-FM construct in the presence of AP. After 24 h, the AP was removed and the construct's localization was determined over time using anti-HA antibodies. As expected, in the presence of AP, Man1-FM was strongly localized to the Golgi as indicated by comparing its staining pattern in the same cells with that of the cis Golgi marker GRASP65 (Fig 3-6A). Similar to our previous observations after induced oligomerization of GPP130 (by either Mn addition for endogenous GPP130 or AP washout for GPP130-FM), Man1-FM clearly redistributed to endosome-like structures. The peripheral punctae were easily detected by 15 min of AP washout and continued to be present while the overall staining became more and more diminished. GRASP65 in the same cells showed no change.

The effect was quantified by determining both the number of punctae per cell (Fig 3-6B) and the total fluorescence per cell (Fig 3-6C). An immunoblotting assay was also used to confirm degradation. As expected, Man1-FM recovery in cell

extracts was strongly diminished upon AP washout (Fig 3-6D) yielding a reduction of over 90% by 5 h (Fig 3-6E). Endogenous GPP130 served as a control and showed no change.

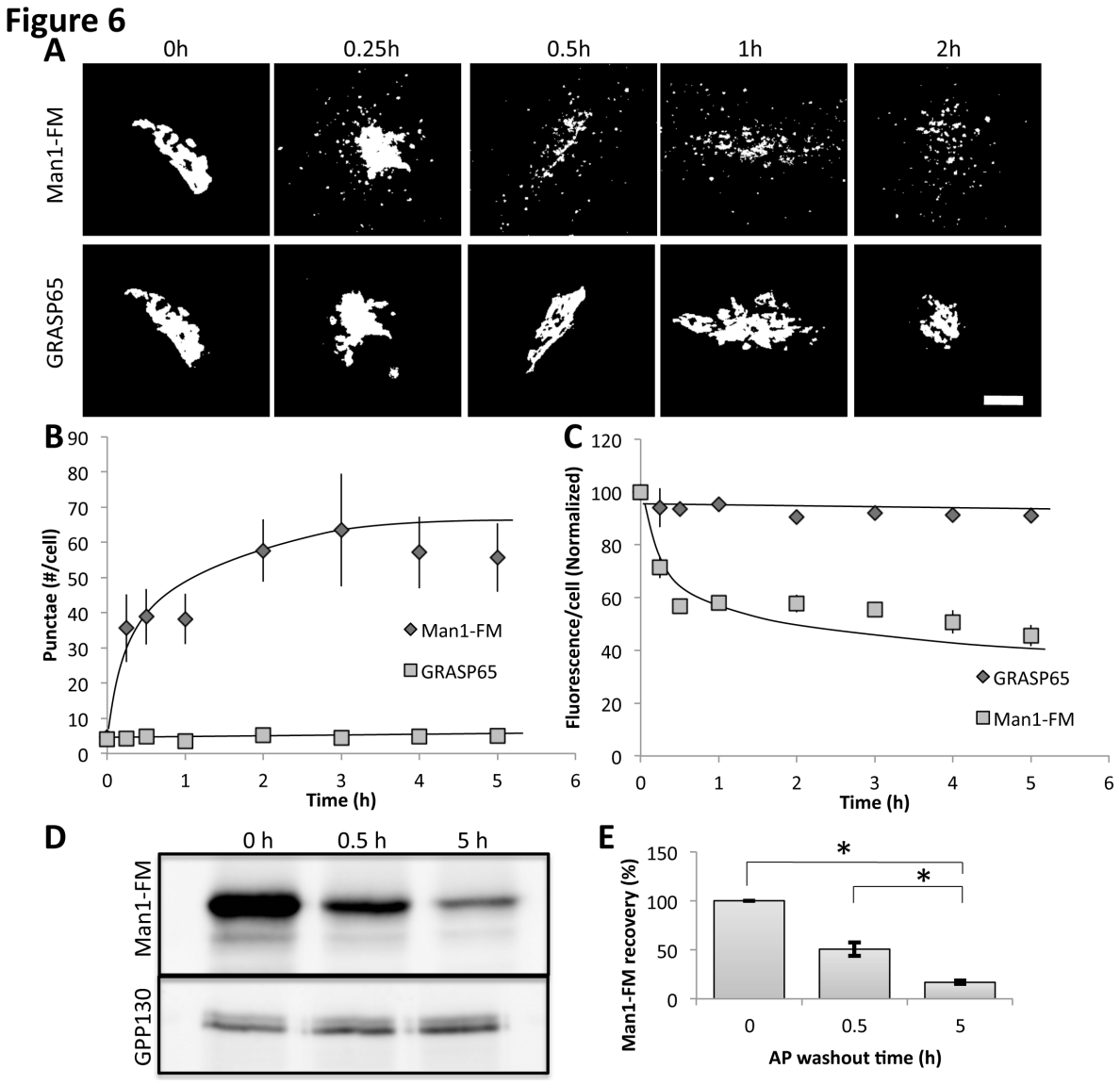

Figure 3-6. Mannosidase-1 leaves the Golgi and is degraded upon oligomerization.

(A) HeLa cells were transiently transfected with Man1-FM in the presence of AP and the AP was washed off for the indicated times to induce polymerization. Thresholded staining of Man1-FM detected using anti-HA antibodies is compared to GRASP65-GFP fluorescence in the same cells.

Bar=5μm. (B) The number of cytoplasmic structures per cell was determined each time point after AP washout for both Man1-FM and the Golgi control GRASP65 using Image J (see Methods). (C) Total cell fluorescence levels of GRASP65 and Man1-FM were determined using ImageJ and normalized to the level of AP treated cells before washout (mean±SEM, n=3, >10 cells per experiment). (D) Immunoblot to determine Man1-FM levels at the indicated times of AP washout with GPP130 detection as loading control. (E) Levels of Man1-FM were quantified at the indicated AP washout time points and normalized to control levels. (mean±SEM, n=3, *p<0.01).

Significantly, redistribution of Man1-FM occurred in cells expressing GGA1 but not GGA1-DN (Fig 3-7A) suggesting it occurs via the same pathway as GPP130. As before, this was confirmed by quantifying appearance in punctae after 1 h of AP washout (Fig 3-7B).

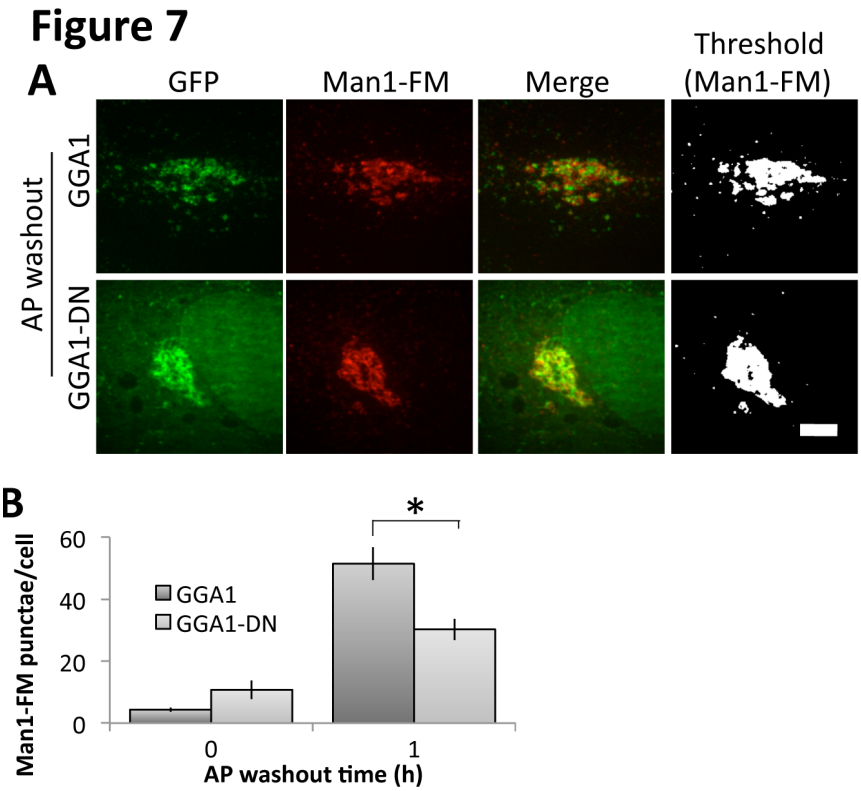

Figure 3-7. GGA1-DN blocks Man1-FM trafficking.

(A) Images show GFP fluorescence of GGA1 or GGA1-DN and anti-HA staining of Man1-FM after 1 h of AP washout. Thresholded Man1-FM staining is also shown. Bar=5μm. (B) The quantified number

of cytoplasmic punctae per cell is shown for Man1-FM at 0 or 1 h after AP wash out (mean±SEM, n=3, >10 cells per experiment, *p<0.05)

Because both Man1 and GPP130 are predominately in the *cis* Golgi at steady state, we next tested whether a *trans* Golgi protein would also respond to oligomerization by leaving the Golgi and undergoing degradation. A similar strategy was used in which the cytoplasmic, transmembrane and stem domains of the *trans* Golgi protein galactosyltransferase (GT) were fused to the tandem array of FM domains followed, in this case, by GFP. Prior to AP washout the construct was strongly Golgi localized but after washout it selectively redistributed to peripheral punctae and, over time, the total GT-FM levels per cell became reduced (Fig 3-8A). These changes were marked compared to giantin in the same cells and both appearance in punctae (Fig 3-8B) and selective loss (Fig 3-8C) were confirmed by image analysis. As expected, degradation was apparent by immunoblot analysis (Fig 3-8D-E).

Figure 8

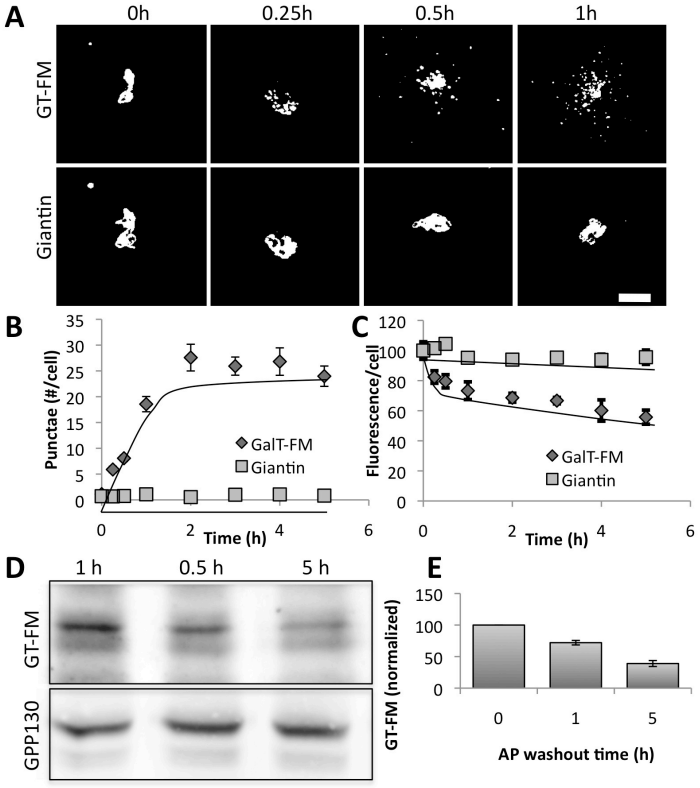

Figure 3-8. Induced oligomerization causes degradation of galactosyltransferase.

(A) Images show thresholded GFP fluorescence of GT-FM and anti-giantin antibody staining after the indicated times of AP washout. Bar=5μm. (B) The quantified number of cytoplasmic punctae per cell is shown for GT-FM and the giantin control at the indicated time points after AP wash out (mean±SEM, n=3, >10 cells per experiment). (C) Total cell fluorescence levels of GT-FM and giantin were determined using ImageJ and normalized to the level of AP treated cells before washout (mean±SEM, n=3, >10 cells per experiment). (D-E) Blot and quantification showing level of GT-FM in cell extracts prepared at the indicated times after AP washout with GPP130 detection as loading control (mean±SEM, n=3).

The lysosome-directed trafficking response is not associated with UPR activation

Given the possibility that the pathway described here is a type of quality control, it seemed important, even if unlikely, to test if our conditions causing oligomerization-induced trafficking of Golgi proteins also activated the unfolded protein response (UPR). For this purpose we assayed upregulation of the ATPase chaperone Bip, which is a standard UPR marker. As a positive control, HeLa cells were treated with tunicamycin to block N-glycosylation and activate the UPR (Oslowski and Urano, 2011). As expected Bip levels increased (Fig 3-9). In contrast, treatment with Mn did not alter Bip levels. To test the effect of AP washout we needed to transfect the cells with GPP130-FM. Transfection frequency was approximately 70% and we noted that transfection alone elevated the level of Bip somewhat. However, AP washout of the transfected cells yielded Bip levels that were identical to cells before AP washout or control transfected cells (Fig 3-9). Therefore, based on Bip level, the UPR was not activated under conditions where oligomerized Golgi proteins are induced to leave the Golgi and undergo degradation. Altogether the experiments here reveal a novel type of quality control in the Golgi in which clustered Golgi proteins are routed for degradation.

Figure 9

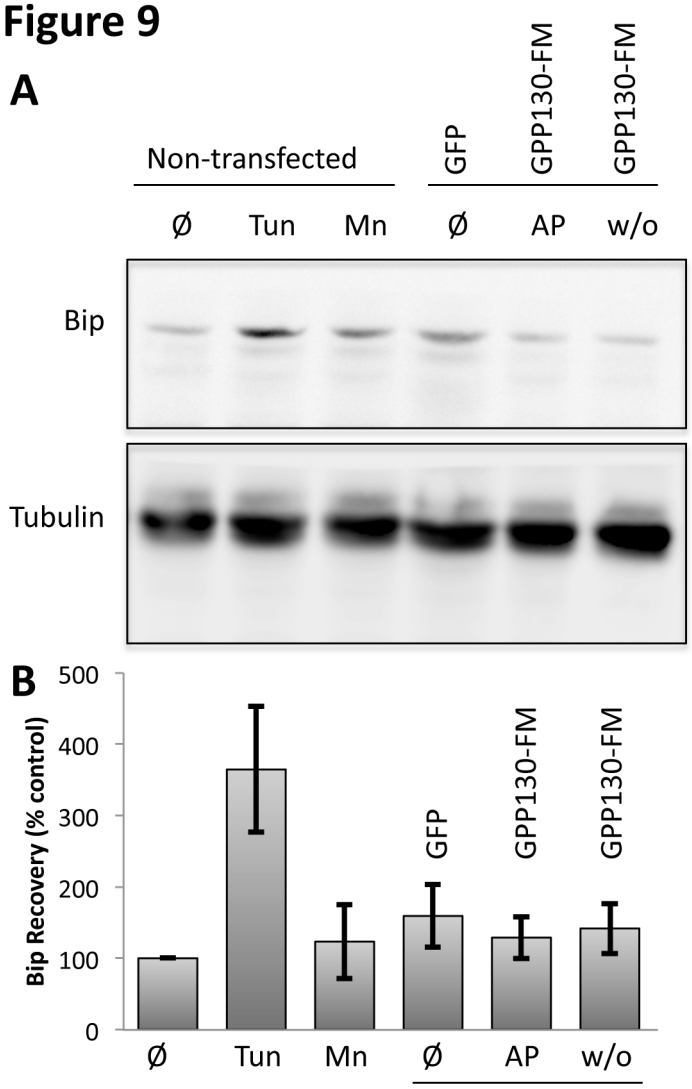

Figure 3-9. Oligomerization-induced trafficking is not associated with UPR activation

(A) Immunoblots using anti-Bip or anti-tubulin antibodies of extracts from non-transfected cells (lanes 1-3) or cells transfected with GPP130-GFP or GPP130-FM (lanes 4-6). The cells were either untreated (Ø), tunicamycin-treated (Tun) to induce the UPR, Mn-treated (Mn) to cause endogenous GPP130 redistribution, left in AP (AP), or subjected to AP washout (w/o) to cause oligomerization of GPP130-FM. (B) Quantification of Bip recovery as a percentage of Bip levels in untreated cells (mean± SEM, n=3).

3.4 Discussion

Our interest in the targeting of Golgi proteins to the lysosome started with Mn-induced degradation of GPP130 (Mukhopadhyay *et al.,* 2010). Subsequently, using mutagenesis, cross-linking, FRAP analysis, and FM-mediated oligomerization we found that Mn oligomerizes GPP130 and that oligomerization is required and sufficient to alter GPP130 trafficking such that it moves from the Golgi to lysosomes where it is degraded (Tewari *et al.,* 2014). Here we report the surprising finding that other, unrelated, Golgi membrane proteins also left the Golgi and were degraded when their oligomerization was induced. Movement of the complexes in an anterograde direction within the Golgi is most easily explained by their size-based exclusion from retrieval vesicles (Rizzo *et al.,* 2013). Interestingly, redistribution and degradation of GPP130 and GPP130-FM are insensitive to nocodazole (our unpublished results and (Mukhopadhyay *et al.,* 2010)) indicating that an intact Golgi ribbon is not required which differs from the intra-Golgi transport of large or aggregated soluble cargo (Lavieu *et al.,* 2014). The requirement for GGA1 and clathrin suggests that upon reaching the TGN, the Golgi protein complexes are engaged by the canonical Golgi-to-lysosome pathway. However, based on GPP130, the sorting appears independent of a cytoplasmic sorting signal raising the possibility that it also involves yet to be described machinery. Elucidating the mechanism of recognition is an important next step, given that it appears to extend to at least several Golgi membrane proteins and for each, it must distinguish between their normal and oligomerized states. Altogether, these observations suggest the

presence of a quality control pathway in the Golgi based on recognition of aggregation state rather than exposure of unfolded domains.

Involvement of the Golgi in quality control, while perhaps underappreciated, is not new. Studies in both yeast and mammalian cells have shown that misfolded proteins may leave the ER before being trafficked back to the ER for dislocation and proteasome-mediated degradation (Hammond and Helenius, 1994; Jenness *et al.*, 1997; Dusseljee *et al.*, 1998; Vashist *et al.*, 2001; Pan *et al.*, 2013; Iannotti *et al.*, 2014) and the UPR upregulates ER-to-Golgi trafficking factors (Travers *et al.*, 2000; Caldwell *et al.*, 2001). Trafficking of selected substrates to the Golgi may assist in ER quality control but the mechanistic basis is poorly understood (Caldwell *et al.*, 2001; Arvan *et al.*, 2002). The proteasome is also involved in turnover of cytoplasmically-disposed Golgi proteins at least under certain conditions (Puthenveedu and Linstedt, 2001). Lysosome mediated degradation of misfolded Golgi proteins has also been observed (Wang *et al.*, 2011). In yeast there is a Golgi-localized ubiquitin ligase, Tul1p, that promotes sorting of mutated proteins with polar transmembrane domains to MVBs (Reggiori and Pelham, 2002). Also, at a non-permissive temperature, the mutated yeast plasma membrane H^+ATPase Pma1p1-7 is targeted directly from the Golgi to the endosomal system for vacuolar degradation (Chang and Fink, 1995). In mammalian cells, certain mutated forms of human lipoprotein lipase fail to be secreted and are targeted from the Golgi to lysosomes for degradation (Busca *et al.*, 1996) and the TGN glycoprotein furin is somehow aggregated by lysosomal protease inhibitors causing its transport to lysosomes (Wolins *et al.*, 1997). Finally, a recent report shows that, under acute ER stress, GPI-linked ERAD substrates traffic

through the Golgi to the cell surface before being degraded in lysosomes (Satpute-Krishnan *et al.,* 2014).

In contrast to all these examples, we assume that the oligomerization/clustering taking place in our experiments is not causing folding defects. The Mn-GPP130 interaction is not yet structurally characterized. But because it is a direct interaction, it presumably involves simultaneous coordination of the metal by GPP130 residues on the outer surface its coiled coil (Tewari *et al.,* 2014). This would cluster the GPP130 dimers without perturbing folding. Similarly, the FM domains we employed are positioned well away from the membrane within the Golgi lumen and undergo a well-characterized interaction with one another. Binding via this mechanism is unlikely to cause folding defects and the UPR was not activated in our experiments. Nevertheless, the FM domain on membrane anchored proteins creates polymers constrained from entering 40-80 nm vesicles and tubules (Rizzo *et al.,* 2013) and capable of stapling single cisternae via lumenal interactions in *trans* (Lavieu *et al.,* 2014).

How might oligomerized/clustered Golgi proteins be differentially recognized by GGA1/clathrin in the TGN? At this point we can only speculate. One thought is that recognition is based on avidity. For the sake of argument, assume that many membrane proteins share a generic determinant that binds weakly to a hypothetical multi-adhesive sorting receptor. Under normal conditions, when the cargo is in its native oligomeric state, the weak interaction with its fast off-rate would yield little sorting. If, on the other hand, the cargo becomes clustered allowing its many copies to simultaneously interact with the multi-adhesive sorting receptor, then sorting

would occur. Given that sorting of GPP130 is independent of its cytoplasmic domain, we would predict a lumenal cargo/receptor interaction and a cytoplasmic receptor/GGA1 interaction. Among known receptors, both mannose-6-phosphate receptors and sortilins use GGA1 and clathrin to mediate Golgi-to-lysosome trafficking of their cargo (Puertollano *et al.,* 2001a; Takatsu *et al.,* 2001; Canuel *et al.,* 2009). While it is important to test the possible role of these receptors, they are not known to act on integral membrane cargo and there is no indication of how they would discriminate between clustered and non-clustered cargo.

Another possibility is differential partitioning of oligomerized cargo in the plane of the membrane. By this view, clusters of transmembrane domains would favor lipid microenvironments that are also recognized by GGA1. Arguably, clustering, if it extends to the transmembrane domains, can impose a rigidity of protein orientation due to mismatch of transmembrane domain length with a given bilayer width. A monomer or dimer with a relatively long transmembrane domain can bury its hydrophobic residues using a skewed orientation but skewing a clustered set of transmembrane domains exacerbates the mismatch. This effect drives a multipass protein containing relatively long transmembrane domains into thicker sections of bilayer (Lin and London, 2013).

A final possibility is that the clustered proteins are travelling to the lysosome by default. That is, the clustered complexes are left behind after all the active sorting events take place at the TGN (including retrieval of their non-clustered counterparts) and that these residual membranes head to MVB/lysosomes. This contradicts the view that the cell surface is the default pathway in mammalian cells. More

importantly, it fails to say anything about the role of GGA1 and clathrin or, more generally, how “default” vesicles acquire targeting and fusion factors necessary for delivery to MVB/lysosomes.

In closing, we have shown that several Golgi proteins leave the Golgi upon oligomerization and are degraded suggesting the presence of an ER independent, Golgi-based quality control system sensitive to oligomeric state. This process would seem to provide another level of quality control in the secretory pathway, in addition to the widely known quality control process in the ER. The primary purpose may be to rid cells of clustered or aggregated proteins that accumulate in the Golgi due to defective Golgi-based processing. The pathway may also prove amenable to manipulations making it therapeutically useful. Oligomerization and the ensuing lysosomal degradation of GPP130 protects against Shiga toxicosis in cultured cells and mice (Mukhopadhyay and Linstedt, 2012). The drug Suramin can aggregate the prion protein PrP in a post-ER/Golgi compartment redirecting it to lysosomes and delaying onset of prion disease (Gilch *et al.,* 2001). Future studies will likely reveal additional components in the oligomer-induced degradation of Golgi proteins providing new potential targets for therapeutic intervention.

3.5 MATERIALS AND METHODS

Antibodies and other reagents. Polyclonal antibodies against GPP130 and giantin, and monoclonal antibodies against GPP130 and GFP have been described earlier (Puri *et al.,* 2002; Mukhopadhyay *et al.,* 2010). For immunoblots, monoclonal anti-HA (Sigma-Aldrich, St. Louis, MO) was used at 1:1000, polyclonal anti-Bip (Abcam®, Cambridge, MA) was used at 1:500, and anti-γ-tubulin (Sigma) was used at 1:1000. Horseradish peroxidase-conjugated goat anti-rabbit or anti-mouse secondary antibodies were used at 1:3000 (Bio-Rad, Hercules, CA). For immunofluorescence, Alexa Fluor 488- and Alexa Fluor 568- (Invitogen, Carlsbad, CA) were used at 1:400. AP (now called D/D solubilizer) was purchased from Clontech (Mountain view, CA). Pitstop®2 was from Abcam® and tunicamycin was from Sigma.

Constructs. GPP130-FM, which contains a GFP tag, is previously described (Tewari *et al.,* 2014). A version substituting an HA tag in place of the GFP tag was used for co-transfection with GGA1 constructs. ∆cyto-GPP130-FM was engineered by looping out residues 2-11 from the 12 residue cytoplasmic domain in GPP130-FM using a polymerase chain reaction-based loop-out modification of the QuikChange protocol (Stratagene, La Jolla, CA), as described (Tewari *et al.,* 2014). Similarly, looping out residues 88-247 from GPP130-FM created GPP130-$_{1\text{-}87}$-FM. Subcloning residues 1-75 of galactosyltransferase in frame before the FM repeats and GFP using Nhe1 and EcoR1 restriction sites generated GT-FM. All constructs were confirmed by restriction analysis and sequencing. GGA1-GFP and GGA1-DN-GFP (Puertollano and Alonso, 1999) were a kind gift from Dr. Juan Bonifacino (National Institutes of Health, Bathesda, MD). GPP130-GFP (residues 1-247) (Mukhopadhyay

et al., 2010) and GRASP65-GFP (Sengupta *et al.,* 2009) have been described previously.

Cell culture and transfection. HeLa cells were grown in minimum essential medium with 100 IU/ml penicillin-G and 100 μg/ml streptomycin (Fisher Scientific, Hanover Park, IL) supplemented with 10% fetal bovine serum (Atlanta Biologicals, Lawrenceville, GA) and maintained at 37°C in a 5% CO_2 incubator. Mn treatment was performed by adding freshly prepared $MnCl_2$ to the culture medium at 500 μM for the indicated times. DNA transfections were performed using the JetPEI® transfection reagent (PolyPlus, Illkirch, France) according to the manufacturer's protocol. Cultures were transfected 24 h after plating and, unless noted otherwise, used for experiments 24 h after transfection. For GGA1 co-expression experiments, only cells expressing moderately high levels of GGA1 and GGA1-DN were analyzed to ensure adequate levels for inhibition by GGA1-DN.

Controlled polymerization. Cells were transfected with the FM constructs and after 16-18 h they were placed in fresh media containing 1μM AP for 24 h. This was followed by another change into media containing 1 μM AP and 100 μg/mL cyclohexamide for 30 minutes. Next, the cells were incubated in media containing only 100 μg/mL cycloheximide for various times of AP washout prior to fixation and imaging. Only cells exhibiting moderate expression levels were analyzed. Note that the control cells contained both cycloheximide and AP throughout the course of the experiment. For the nocodazole experiments, HeLa cells were treated with 1 μg/mL nocodazole and 100 μg/mL cycloheximide for 3h, followed by either Mn addition for

1h or 5h or AP removal for 1 h in GPP130-FM transfected cells. Nocodazole and cycloheximide were present during the entire course of the experiment. For Pitstop®2 experiments, 24 h post transfection, the GPP130-FM transfected cells were serum deprived for 45 min in the presence of AP, followed by AP washout for 10 min in the presence of Pitstop®2 (30 μM) in DMSO or DMSO alone. Note that we also confirmed that this period of serum deprivation did not affect GPP130-FM redistribution to endosomal punctae.

Immunoblot analysis. HeLa cells from 60 mm plates were harvested in Tris-SDS lysis buffer (25 mM Tris-Cl, pH 6.7, 1.5% SDS, 0.1% β-mercaptoethanol, and 1 mM phenylmethanesulfonylfluoride), passed through a 25-gauge needle ~10 times, and clarified by centrifugation at 15,000 rpm for 15 minutes at 4°C. Protein levels were determined using the Pierce® BCA protein assay (Thermo Scientific, Waltham, MA) and equal protein amounts of lysate were analyzed by SDS PAGE and immunoblotting. Immunoblots were quantified using ImageGauge software (Fujifilm, Valhalla, NY). For Man1-FM, transfected cells were subjected to AP washout for 0, 0.5, or 5 h before lysis. For Bip assays, cells were treated for 6 h with 3 μM tunicamycin, 500 μM Mn, or a washout of AP from GPP130-FM transfected cells.

Microscopy and image analysis. Immunofluorescence on 3% PFA fixed cells was performed exactly as described (Tewari *et al.,* 2014) using a spinning-disk confocal microscope and sectioning at 0.3 μm steps. Display images are maximum value projections excepting those that are thresholded to highlight cytoplasmic punctae. For these, a uniform threshold was applied after background subtraction. The

images were analyzed using ImageJ (National Institutes of Health, Bethesda, MD, http://imagej.nih.gov/ij/) as described (Tewari *et al.,* 2014). To measure fluorescence per cell, background was subtracted from each Z section and average value projections were created. Cells were outlined using the Gaussian blur filter and mean fluorescence was measured using the Measure plugin of ImageJ. The number of cytoplasmic punctae per cell was determined using the Analyze Particle plugin of ImageJ (particle range setting of 10-100 pixels) from maximum value projections that were uniformly thresholded after background subtraction. For all experiments, data are presented as averages of 3 experiments with at least 10 cells per condition per experiment. For total fluorescence, the data were normalized using the control values. Comparisons between two groups were performed using two-tailed Student's t test assuming equal variances. In general, $p < 0.05$ was considered significant and the determined *p* values are provided in the figure legends. Asterisks (*) in graphs, wherever present, denote statistically significant differences.

3.6 REFERENCES

Arvan, P., Zhao, X., Ramos-Castaneda, J., and Chang, A. (2002). Secretory pathway quality control operating in Golgi, plasmalemmal, and endosomal systems. Traffic *3*, 771-780.

Bachert, C., Lee, T.H., and Linstedt, A.D. (2001). Lumenal endosomal and Golgi-retrieval determinants involved in pH-sensitive targeting of an early Golgi protein. Mol Biol Cell *12*, 3152-3160.

Beddoe, T., Paton, A.W., Le Nours, J., Rossjohn, J., and Paton, J.C. (2010). Structure, biological functions and applications of the AB5 toxins. Trends Biochem Sci *35*, 411-418.

Black, M.W., and Pelham, H.R. (2000). A selective transport route from Golgi to late endosomes that requires the yeast GGA proteins. J Cell Biol *151*, 587-600.

Bonifacino, J.S., and Glick, B.S. (2004). The mechanisms of vesicle budding and fusion. Cell *116*, 153-166.

Brown, M.S., and Goldstein, J.L. (1997). The SREBP pathway: regulation of cholesterol metabolism by proteolysis of a membrane-bound transcription factor. Cell *89*, 331-340.

Bucci, C., Thomsen, P., Nicoziani, P., McCarthy, J., and van Deurs, B. (2000). Rab7: a key to lysosome biogenesis. Mol Biol Cell *11*, 467-480.

Busca, R., Martinez, M., Vilella, E., Pognonec, P., Deeb, S., Auwerx, J., Reina, M., and Vilaro, S. (1996). The mutation Gly142-->Glu in human lipoprotein lipase produces a missorted protein that is diverted to lysosomes. J Biol Chem *271*, 2139-2146.

Caldwell, S.R., Hill, K.J., and Cooper, A.A. (2001). Degradation of endoplasmic reticulum (ER) quality control substrates requires transport between the ER and Golgi. J Biol Chem *276*, 23296-23303.

Canuel, M., Libin, Y., and Morales, C.R. (2009). The interactomics of sortilin: an ancient lysosomal receptor evolving new functions. Histol Histopathol *24*, 481-492.

Chang, A., and Fink, G.R. (1995). Targeting of the yeast plasma membrane [H+]ATPase: a novel gene AST1 prevents mislocalization of mutant ATPase to the vacuole. J Cell Biol *128*, 39-49.

Dusseljee, S., Wubbolts, R., Verwoerd, D., Tulp, A., Janssen, H., Calafat, J., and Neefjes, J. (1998). Removal and degradation of the free MHC class II beta chain in the endoplasmic reticulum requires proteasomes and is accelerated by BFA. J Cell Sci *111 (Pt 15)*, 2217-2226.

Gilch, S., Winklhofer, K.F., Groschup, M.H., Nunziante, M., Lucassen, R., Spielhaupter, C., Muranyi, W., Riesner, D., Tatzelt, J., and Schatzl, H.M. (2001). Intracellular re-routing of prion protein prevents propagation of PrP(Sc) and delays onset of prion disease. EMBO J *20*, 3957-3966.

Hammond, C., and Helenius, A. (1994). Quality control in the secretory pathway: retention of a misfolded viral membrane glycoprotein involves cycling between the ER, intermediate compartment, and Golgi apparatus. J Cell Biol *126*, 41-52.

He, X., Chang, W.P., Koelsch, G., and Tang, J. (2002). Memapsin 2 (beta-secretase) cytosolic domain binds to the VHS domains of GGA1 and GGA2: implications on the endocytosis mechanism of memapsin 2. FEBS Lett *524*, 183-187.

Iannotti, M.J., Figard, L., Sokac, A.M., and Sifers, R.N. (2014). A Golgi-localized mannosidase (MAN1B1) plays a non-enzymatic gatekeeper role in protein biosynthetic quality control. J Biol Chem *289*, 11844-11858.

Irannejad, R., and von Zastrow, M. (2014). GPCR signaling along the endocytic pathway. Curr Opin Cell Biol *27*, 109-116.

Jenness, D.D., Li, Y., Tipper, C., and Spatrick, P. (1997). Elimination of defective alpha-factor pheromone receptors. Mol Cell Biol *17*, 6236-6245.

Lavieu, G., Dunlop, M.H., Lerich, A., Zheng, H., Bottanelli, F., and Rothman, J.E. (2014). The Golgi ribbon structure facilitates anterograde transport of large cargoes. Mol Biol Cell *25*, 3028-3036.

Le Gall, S., Erdtmann, L., Benichou, S., Berlioz-Torrent, C., Liu, L., Benarous, R., Heard, J.M., and Schwartz, O. (1998). Nef interacts with the mu subunit of clathrin adaptor complexes and reveals a cryptic sorting signal in MHC I molecules. Immunity *8*, 483-495.

Lin, Q., and London, E. (2013). Altering hydrophobic sequence lengths shows that hydrophobic mismatch controls affinity for ordered lipid domains (rafts) in the multitransmembrane strand protein perfringolysin O. J Biol Chem *288*, 1340-1352.

Linstedt, A.D., Mehta, A., Suhan, J., Reggio, H., and Hauri, H.P. (1997). Sequence and overexpression of GPP130/GIMPc: evidence for saturable pH-sensitive targeting of a type II early Golgi membrane protein. Mol Biol Cell *8*, 1073-1087.

Mukhopadhyay, S., Bachert, C., Smith, D.R., and Linstedt, A.D. (2010). Manganese-induced trafficking and turnover of the cis-Golgi glycoprotein GPP130. Mol Biol Cell *21*, 1282-1292.

Mukhopadhyay, S., and Linstedt, A.D. (2012). Manganese blocks intracellular trafficking of Shiga toxin and protects against Shiga toxicosis. Science *335*, 332-335.

Mukhopadhyay, S., Redler, B., and Linstedt, A.D. (2013). Shiga toxin-binding site for host cell receptor GPP130 reveals unexpected divergence in toxin-trafficking mechanisms. Mol Biol Cell *24*, 2311-2318.

Natarajan, R., and Linstedt, A.D. (2004). A cycling cis-Golgi protein mediates endosome-to-Golgi traffic. Mol Biol Cell *15*, 4798-4806.

Oslowski, C.M., and Urano, F. (2011). Measuring ER stress and the unfolded protein response using mammalian tissue culture system. Methods Enzymol *490*, 71-92.

Pan, S., Cheng, X., and Sifers, R.N. (2013). Golgi-situated endoplasmic reticulum alpha-1, 2-mannosidase contributes to the retrieval of ERAD substrates through a direct interaction with gamma-COP. Mol Biol Cell *24*, 1111-1121.

Piper, R.C., Dikic, I., and Lukacs, G.L. (2014). Ubiquitin-dependent sorting in endocytosis. Cold Spring Harb Perspect Biol *6*.

Polishchuk, R., and Lutsenko, S. (2013). Golgi in copper homeostasis: a view from the membrane trafficking field. Histochem Cell Biol *140*, 285-295.

Puertollano, R., Aguilar, R.C., Gorshkova, I., Crouch, R.J., and Bonifacino, J.S. (2001a). Sorting of mannose 6-phosphate receptors mediated by the GGAs. Science *292*, 1712-1716.

Puertollano, R., and Alonso, M.A. (1999). MAL, an integral element of the apical sorting machinery, is an itinerant protein that cycles between the trans-Golgi network and the plasma membrane. Mol Biol Cell *10*, 3435-3447.

Puertollano, R., Randazzo, P.A., Presley, J.F., Hartnell, L.M., and Bonifacino, J.S. (2001b). The GGAs promote ARF-dependent recruitment of clathrin to the TGN. Cell *105*, 93-102.

Puri, S., Bachert, C., Fimmel, C.J., and Linstedt, A.D. (2002). Cycling of early Golgi proteins via the cell surface and endosomes upon lumenal pH disruption. Traffic *3*, 641-653.

Puthenveedu, M.A., and Linstedt, A.D. (2001). Evidence that Golgi structure depends on a p115 activity that is independent of the vesicle tether components giantin and GM130. J Cell Biol *155*, 227-238.

Reggiori, F., and Pelham, H.R. (2002). A transmembrane ubiquitin ligase required to sort membrane proteins into multivesicular bodies. Nat Cell Biol *4*, 117-123.

Rizzo, R., Parashuraman, S., Mirabelli, P., Puri, C., Lucocq, J., and Luini, A. (2013). The dynamics of engineered resident proteins in the mammalian Golgi complex relies on cisternal maturation. J Cell Biol *201*, 1027-1036.

Roeth, J.F., Williams, M., Kasper, M.R., Filzen, T.M., and Collins, K.L. (2004). HIV-1 Nef disrupts MHC-I trafficking by recruiting AP-1 to the MHC-I cytoplasmic tail. J Cell Biol *167*, 903-913.

Satpute-Krishnan, P., Ajinkya, M., Bhat, S., Itakura, E., Hegde, R.S., and Lippincott-Schwartz, J. (2014). ER stress-induced clearance of misfolded GPI-anchored proteins via the secretory pathway. Cell *158*, 522-533.

Sengupta, D., Truschel, S., Bachert, C., and Linstedt, A.D. (2009). Organelle tethering by a homotypic PDZ interaction underlies formation of the Golgi membrane network. J Cell Biol *186*, 41-55.

Starr, T., Forsten-Williams, K., and Storrie, B. (2007). Both post-Golgi and intra-Golgi cycling affect the distribution of the Golgi phosphoprotein GPP130. Traffic *8*, 1265-1279.

Sun, L.P., Seemann, J., Goldstein, J.L., and Brown, M.S. (2007). Sterol-regulated transport of SREBPs from endoplasmic reticulum to Golgi: Insig renders sorting signal in Scap inaccessible to COPII proteins. Proc Natl Acad Sci U S A *104*, 6519-6526.

Surma, M.A., Klose, C., and Simons, K. (2012). Lipid-dependent protein sorting at the trans-Golgi network. Biochim Biophys Acta *1821*, 1059-1067.

Takatsu, H., Katoh, Y., Shiba, Y., and Nakayama, K. (2001). Golgi-localizing, gamma-adaptin ear homology domain, ADP-ribosylation factor-binding (GGA) proteins interact with acidic dileucine sequences within the cytoplasmic domains of sorting receptors through their Vps27p/Hrs/STAM (VHS) domains. J Biol Chem *276*, 28541-28545.

Tartakoff, A.M. (1983). Perturbation of vesicular traffic with the carboxylic ionophore monensin. Cell *32*, 1026-1028.

Tewari, R., Jarvela, T., and Linstedt, A.D. (2014). Manganese induces oligomerization to promote down-regulation of the intracellular trafficking receptor used by Shiga toxin. Mol Biol Cell *25*, 3049-3058.

Traub, L.M., and Bonifacino, J.S. (2013). Cargo recognition in clathrin-mediated endocytosis. Cold Spring Harb Perspect Biol *5*, a016790.

Travers, K.J., Patil, C.K., Wodicka, L., Lockhart, D.J., Weissman, J.S., and Walter, P. (2000). Functional and genomic analyses reveal an essential coordination between the unfolded protein response and ER-associated degradation. Cell *101*, 249-258.

Vanlandingham, P.A., and Ceresa, B.P. (2009). Rab7 regulates late endocytic trafficking downstream of multivesicular body biogenesis and cargo sequestration. J Biol Chem *284*, 12110-12124.

Vashist, S., Kim, W., Belden, W.J., Spear, E.D., Barlowe, C., and Ng, D.T. (2001). Distinct retrieval and retention mechanisms are required for the quality control of endoplasmic reticulum protein folding. J Cell Biol *155*, 355-368.

von Kleist, L.,Stahlschmidt, W., Bulut, H., Gromova,K., Puchkov,D., Robertson, M.J., MacGregor, K.A., Tomilin, N., Pechstein, A., Chau, N., Chircop, M., Sakoff, J., von Kries, J.P., Saenger, W., Krausslich, H.G., Shupliakov, O., Robinson, P.J., McCluskey, A., and Haucke, V. (2011). Role of the clathrin terminal domain in regulating coated pit dynamics revealed by small molecule inhibition. Cell 146, 471-484.

Wolins, N., Bosshart, H., Kuster, H., and Bonifacino, J.S. (1997). Aggregation as a determinant of protein fate in post-Golgi compartments: role of the luminal domain of furin in lysosomal targeting. J Cell Biol *139*, 1735-1745.

Zhu, Y., Doray, B., Poussu, A., Lehto, V.P., and Kornfeld, S. (2001). Binding of GGA2 to the lysosomal enzyme sorting motif of the mannose 6-phosphate receptor. Science *292*, 1716-1718.

CHAPTER 4

CONCLUSIONS AND FUTURE DIRECTIONS

4.1 SUMMARY

This project, which started with investigating the trafficking paradigm of the *cis* Golgi GPP130, revealed metal-induced oligomerization as a sorting mechanism and the potential role of the Golgi in protein quality control. Mutagenesis narrowed a transferable Mn responsive trafficking determinant to about 50 residues (residues 50-100) in the predicted coiled-coil and, more importantly, alanine scanning identified a required stretch of residues ^{88}DFLV^{91}, which upon alanine substitution blocked Mn binding, oligomerization and trafficking to lysosomes. Inhibition of GGA1 specifically blocked GPP130 redistribution suggesting that the redistribution of oligomeric GPP130 to lysosomes uses the canonical route of Golgi-to-lysosomes trafficking.

Furthermore, using a drug-controlled reversibly polymerizable version of GPP130, we discovered that oligomerization of GPP130 is sufficient to target it to lysosomes in a GGA1 and clathrin dependent route. Unexpectedly, neither the cytoplasmic tail nor sequence determinants in its predicted coiled-coil domain critical for normal cycling or Mn sensitivity were required for this movement. This strongly suggested the presence of a general mechanism in the Golgi that can distinguish between the native and aggregated states of proteins. This startling result prompted us to assay any change in sorting at the TGN of other unrelated Golgi proteins in response to oligomerization. Surprisingly, we observed that two other unrelated Golgi membrane proteins, *cis* Golgi localized mannosidase 1 (Man1) and *trans* Golgi

localized galactosyltransferase (GT), were also targeted for lysosomal degradation upon their oligomerization. This process was also GGA1 dependent. Microtubules and an intact Golgi ribbon were not required for this movement, which occurred in the absence of a detectable ER-based UPR activation.

Significantly, these data reflect upon an underappreciated role of the Golgi in what seems like a protein quality control process that may be useful in generating therapies designed to down-regulate specific proteins in the secretory pathway. A Golgi-based quality control would be clearly valuable in cases where misfolded proteins either escape the ER or arise in post-ER compartments. From an evolutionary perspective, the GPP130 response to elevated Mn levels, which may play a role in Mn homeostasis, may have arisen by using a pre-existing quality control pathway.

4.2 FUTURE DIRECTIONS

Characterization of the interaction between Mn and GPP130

Despite an improved understanding of the mechanism of manganese-induced trafficking of GPP130, several questions remain to be answered. While we have shown direct binding between GPP130 and Mn in vitro with an estimated dissociation constant of 0.4mM, we are unaware of how Mn is co-coordinated by GPP130 and how many Mn ions bind each GPP130 dimer. There are no canonical Mn binding sites in GPP130 and the identified ^{88}DFLV^{91} sequence in the stem domain gives little clue on the nature of binding. The aspartate in the DFLV sequence is of particular interest given its participation in a number of metal interactions. Indeed, most known Mn binding sites across kingdoms include negatively charged (Glu/Asp) and histidine

residues. For instance, in human SOD (superoxide dismutase, a homotetramer of 22kDa), MnII is part of the active site and is coordinated by three histidine ligands (His 26, 74, and 163), one aspartate (Asp 159) and a water molecule or hydroxide as a fifth ligand in a compact trigonal bipyramidal geometry (Borgstahl et al., 1992). The binding site that we discovered includes a negatively charged aspartate residue but doesn't involve any histidine residues, although there are neighboring histidine residues at positions 67 and 82 which may aid in reinforcing the binding. As discussed in section 2.3, since the Mn binding to GPP130 appears weak, most likely the Mn ion may be partially coordinated by engaging with the side chains of the residues DFLV, triggering linking between distinct GPP130-coiled coils to achieve full coordination and promoting aggregation in the process.

It is important to note here that we cannot rule out the possibility of multiple Mn binding sites in GPP130. The predicted coiled-coil domain of GPP130 is divided into 3 subdomains (G1, XA, G2) containing independently acting Golgi (G1, G2) and endosome localization determinants (XA) (Bachert et al., 2001), and at least two subdomains are required in conjunction with a cis Golgi targeting motif to be Mn-trafficking competent (Mukhopadhyay et al., 2010). The experiments in this study focused on the subdomains G1 (residues 36-87) and XA (residues 88-175). There might be additional Mn binding sites in G2 (residues 176-245), in the light of constructs containing G1 and G2 (residues 36-87_176-247) as well as XA and G2 (residues 88-247) being Mn trafficking competent (Mukhopadhyay et al., 2010). A detailed description of Mn binding by the GPP130 stem domain using techniques like Nuclear Magnetic Resonance or other spectroscopic methods such as Electron

Paramagnetic Resonance is an important future direction. Unfortunately, our attempts to date were not fruitful due to low yields of purified GPP130 protein. Use of a small Mn-binding peptide from GPP130 that retains its coiled-coil character or troubleshooting ways to increase protein yield will circumvent this problem.

Testing the role of GPP130 In Mn homeostasis

The regular function of GPP130 is unclear and we speculate that it might play a pivotal role in Mn homeostasis in mammalian cells. GPP130 is the only known Golgi protein to be down-regulated by Mn and Mn is the only divalent ion that affects its trafficking (Mukhopadhyay et al., 2010). However, we have not tested this role of GPP130.

Increased Mn transport into the Golgi has been previously shown to protect cells against Mn-induced cytotoxicity (Mukhopadhyay and Linstedt, 2011). On the other hand, blocking Mn transport into the Golgi or out of the Golgi to the cell surface has the opposite effect, thus showing the importance of the Golgi apparatus in Mn homeostasis and detoxification in mammalian cells (Mukhopadhyay, S., and Linstedt, A.D., 2011). An attractive hypothesis is that GPP130 acts as a negative regulator of the Golgi localized Mn pump, Secretory Pathway Ca ATPase1 or SPCA1, and perhaps directly modulates its activity. SPCA1 pumps Mn from the cytosol into the Golgi for secretion to maintain cytosolic levels of Mn (Fairclough et al., 2003; Mukhopadhyay, and Linstedt, 2011). When extracellular Mn levels are low, SPCA1-mediated movement of Mn into the Golgi may be diminished by GPP130 to maintain basal levels of cytosolic Mn. In contrast, elevated concentrations of Mn may require amplification of the activity of SPCA1 to pump more Mn into the Golgi for subsequent

secretion and maintenance of Mn homeostasis. If this were the case, it would seem befitting to eliminate GPP130 in light of elevated Mn levels, to accelerate Mn sequestration into the Golgi for secretion. GPP130 could interact with a newly synthesized pool of SPCA1 transiting through the Golgi and regulate its trafficking in a Mn dependent manner. Thus, it will be important to test for an interaction between SPCA1 and GPP130.

Alternately, GPP130 could regulate the trafficking of a newly synthesized pool of an Mn transporter transiting the Golgi en route to the plasma membrane. It might bind the transporter and direct it to lysosomes in response to elevated Mn. This would control Mn entry into the cell. However, this seems highly unlikely since Mn enters into mammalian cells via a range of diverse transporters, pumps and channels that are neither specific for Mn ions nor regulated by its intracellular levels (Au et al., 2008). Overall, it is expected that identification of the interacting partners of GPP130, in the presence and absence of Mn, will fill the gaps in our understanding of the missing mechanistic details of the Mn regulation of GPP130 and the purpose of Mn-induced GPP130 degradation.

Oligomerization of Golgi proteins directs them to lysosomes for degradation

We made a startling discovery that induced oligomerization of Golgi membrane proteins altered their trafficking leading to their degradation. This process appears to extend over several Golgi membrane proteins (GPP130, Man1, GT) and somehow differentiate between their native and oligomeric states, reminiscent of a protein quality control process. A key next step is to determine how these oligomeric proteins

are recognized and marked for lysosomal sorting. More simply, how does oligomerization alter sorting?

An important component in understanding the mechanistic details of this process is to characterize the interaction of the oligomerized proteins with GGA1. GGA1 usually interacts with acidic-cluster dileucine motifs in the cytoplasmic domain of cargo protein (Puertollano et al., 2001). The dispensable nature of the cytoplasmic tail of GPP130 makes it difficult to reconcile how oligomerized GPP130 interacts with GGA1. Most likely GGA1 interacts indirectly with GPP130 through a sorting receptor that somehow selectively binds the oligomerized protein. We expect this protein to be an integral membrane protein with its lumenal domain recognizing the oligomerized protein and cytosolic tail engaging GGA1.

A candidate for the role of the sorting receptor is sortilin, the mammalian homologue of Vps10p. Vps10p in the yeast late Golgi recognizes a wide variety of sequence determinants, some of which have the qualities of extended-flexible polypeptides instead of specific peptide motifs and directs them to the vacuole for degradation (Hong et al., 1996; Jørgensen et al., 1999). Because of this degeneracy in vacuolar sorting signals, Vps10p has been suggested to function as a quality control cargo receptor that recognizes aberrant proteins in the Golgi lumen and directs them to the vacuole for degradation (Hong et al., 1996). Sortilin contains a cysteine rich lumenal domain homologous to Vps10p that recognizes cargo proteins and a cytoplasmic tail containing two endosome/lysosome sorting motifs (acidic dileucine and tyrosine-based) that engages adaptor proteins (Nykjaer et al, 2012; Nielsen et al., 2001). Significantly, sortilin has been implicated in TGN to lysosome trafficking of

cargo and its cytoplasmic tail has been shown to interact with GGA1 at the TGN (Takatsu et al, 2001) making it a prime candidate for role of the sorting receptor. Furthermore, sortilin recognizes several unrelated ligands implying flexibility in the recognition of cargo sorting signals similar to Vps10p (Nielsen et al., 2001; Gelling et al., 2012). However, so far sortilin has only been implicated in the sorting of soluble ligands (Canuel et al., 2009). Testing the effect of loss of sortilin on the trafficking of oligomerized Golgi proteins could provide insight into how they are sorted.

Alternately, a less direct approach employing immunoprecipitation of the oligomerized proteins followed by mass-spectrometry should identify components in addition to GGA1 and clathrin that participate in the sorting.

In conclusion, there are exciting avenues to extend the work reported, which already provides a paradigm for metal-regulated protein sorting and identifies a pathway for apparent quality control of Golgi proteins.

4.3 REFERENCES

Au, C., Benedetto, A., and Aschner, M. (2008). Manganese in eukaryotes. Neurotoxicology 29, 569–576.

Bachert, C., Lee, T.H., and Linstedt, A.D. (2001) Lumenal endosomal and Golgi-retrieval determinants involved in pH-sensitive targeting of an early Golgi protein. Molecular biology of the cell 12(10): 3152-3160.

Borgstahl, G.E., Parge, H.E., Hickey, M.J., Beyer, W.F., Jr., Hallewell, R.A., and Tainer, J.A. (1992). The structure of human mitochondrial manganese superoxide dismutase reveals a novel tetrameric interface of two 4-helix bundles. Cell *71*, 107-118.

Canuel, M., Libin, Y., and Morales, C. R. (2009). The interactomics of sortilin: an ancient lysosomal receptor evolving new functions. Histol Histopathol 24: 481-492

Fairclough, R.J., Dode, L., Vanoevelen, J., Andersen, J.P., Missiaen J., Raeymaekers, L., Wuytack, F., and Hovnanian, A. (2003). Effect of Hailey-Hailey disease mutations on the function of a new variant of human secretory pathway Ca2+/Mn2+-ATPase (hSPCA1). J Biol Chem, 278:24721–24730.

Gelling, C. L., Dawes, I. W., Perlmutter, D. H., Fisher, E. A., & Brodsky, J. L. (2012). The Endosomal Protein-Sorting Receptor Sortilin Has a Role in Trafficking a-1 Antitrypsin. Genetics, 192, 889-903.

Hong, E., Davidson, A.R., and Kaiser, C.A. (1996). A Pathway for Targeting Soluble Misfolded Proteins to the Yeast Vacuole. The Journal of Cell Biology, Volume 135, Number 3, November 1996 623-633.

Jørgensen, M. U., Emr, S. D. and Winther, J. R. (1999), Ligand recognition and domain structure of Vps10p, a vacuolar protein sorting receptor in *Saccharomyces cerevisiae*. European Journal of Biochemistry, 260: 461–469.

Mukhopadhyay, S., Bachert, C., Smith, D. R. and Linstedt, A. D (2010). Manganese induced trafficking and turnover of the cis-Golgi glycoprotein GPP130. Mol Biol Cell 21, 1282-1292.

Mukhopadhyay, S., and Linstedt, A.D. (2011). Identification of a gain-of-function mutation in a Golgi P-type ATPase that enhances Mn2+ efflux and protects against toxicity. Proc Natl Acad Sci U S A, 108, 858-863.

Mukhopadhyay, S., and Linstedt, A., D. (2012). Manganese blocks intracellular trafficking of Shiga toxin and protects against Shiga toxicosis. Science, 335(6066): 332-335.

Nielsen, M. S., Madsen, P., Christensen, E. I., Nykjær, A., Gliemann, J., Kasper, D., Pohlmann, R., & Petersen, C. M. (2001). The sortilin cytoplasmic tail conveys Golgi–endosome transport and binds the VHS domain of the GGA2 sorting protein. The EMBO Journal, 20(9), 2180-2190.

Nykjaer, A., & Willnow, T. E. (2012). Sortilin: a receptor to regulate neuronal viability and function. Trends in neurosciences, *35*(4), 261-270.

Puertollano, R., Aguilar, R.C., Gorshkova, I., Crouch, R.J., and Bonifacino, J.S. (2001). Sorting of mannose 6-phosphate receptors mediated by the GGAs. Science 292, 1712-1716.

Takatsu, H., Katoh, Y., Shiba Y., and Nakayama, K. (2001). Golgi-localizing, γ-Adaptin Ear Homology Domain, ADP-ribosylation Factor-binding (GGA) Proteins Interact with Acidic Dileucine Sequences within the Cytoplasmic Domains of Sorting Receptors through Their Vps27p/Hrs/STAM (VHS) Domains. J. Biol. Chem. 2001 276: 28541-28545.